General Disclaimer

One or more of the Following Statements may affect this Document

- This document has been reproduced from the best copy furnished by the organizational source. It is being released in the interest of making available as much information as possible.

- This document may contain data, which exceeds the sheet parameters. It was furnished in this condition by the organizational source and is the best copy available.

- This document may contain tone-on-tone or color graphs, charts and/or pictures, which have been reproduced in black and white.

- This document is paginated as submitted by the original source.

- Portions of this document are not fully legible due to the historical nature of some of the material. However, it is the best reproduction available from the original submission.

Produced by the NASA Center for Aerospace Information (CASI)

DYNAMICS OF TOWED DECELERATORS

By

James Franklin Campbell

Thesis submitted to the Graduate Faculty of the

Virginia Polytechnic Institute

in partial fulfillment for the degree of

MASTER OF SCIENCE

in

AEROSPACE ENGINEERING

January 1968

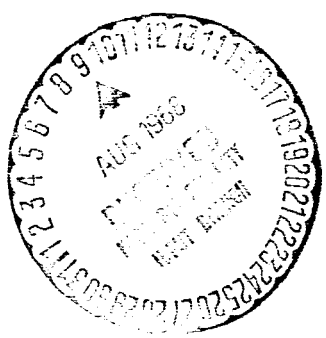

N 69-19898

(ACCESSION NUMBER) (THRU)

67 1

(PAGES) (CODE)

TMX # 61528 02

(NASA CR OR TMX OR AD NUMBER) (CATEGORY)

FACILITY FORM 602

DYNAMICS OF TOWED DECELERATORS

By

James Franklin Campbell

ABSTRACT

A preliminary investigation has been undertaken to theoretically determine the geometric and aerodynamic parameters which have the greatest influence on the stability and performance of the nonporous towed decelerator. To aid in this endeavor a mathematical model was generated to describe the flexible tow line - decelerator dynamical system as a rigid two-body problem. The resulting second-order governing differential equations of motion were used to obtain the characteristic equation (quartic) describing the coupled motions of the two bodies. Evaluation of the coefficients of the quartic yielded expressions which illustrate when the dynamical system is unquestionably unstable.

The two single-degree of freedom cases investigated were the motion of the decelerator about its nose and the motion of the rod and decelerator about the pivot point. For both of these cases expressions were derived for the natural angular frequency, damping factor, steady-state solution, and time to damp to one-half amplitude. Specific comments were made concerning a conical shaped decelerator to illustrate some of the geometric and aerodynamic parameters affecting the spring constant and the natural angular frequency. The boundary between stability and instability was obtained for these two single-degree of freedom cases.

DYNAMICS OF TOWED DECELERATORS

by

James Franklin Campbell

Thesis submitted to the Graduate Faculty of the

Virginia Poly echnic Institute

in partial fulfillment for the degree of

MASTER OF SCIENCE

in

AEROSPACE ENGINEERING

APPROVED: F. R. DeJarnette
Chairman

Frederick Fritze

Wm. P. Harrison

Date

January 1968

Blacksburg, Virginia

I. TABLE OF CONTENTS

II. ACKNOWLEDGMENTS

The author wishes to express his appreciation to the National Aeronautics and Space Administration for the permission to perform analytical research on this thesis during duty hours. He also wishes to thank Dr. Fred R. DeJarnette and Dr. Frederick H. Lutze of the Aerospace Engineering Department of the Virginia Polytechnic Institute for their helpful comments and advice in the preparation of this thesis.

III. LIST OF FIGURES

IV. INTRODUCTION

Advent of super- and hypersonic aircraft, missiles, and spacecraft has dictated the need for adequate deceleration systems capable of performing emergency rescue and/or payload recovery. For example, rescue of a pilot ejecting from his aircraft or spacecraft at extremely high speeds is dependent on some decelerator system to stabilize him and to slow his fall to the point where a conventional terminal descent system, such as a parachute, can be utilized. Also, the success of a mission to place an instrument package on the surfaces of Venus and Mars largely depends on proper deceleration of the payload through their respective atmospheres. One such system being considered to perform these types of missions is the towed deployable decelerator which utilizes aerodynamic drag to decelerate and stabilize the payload or capsule. Two of the approaches made in designing towed decelerators required to function at supersonic and hypersonic speeds are: (1) adaption of existing subsonic parachute configurations and (2) generation of nonporous inflatable bodies having specific geometric shapes. Of these two approaches, the nonporous body inflated either by compressed gas or by ram-air (inlets) presently appears to provide the more promising approach to high-speed deceleration problems, as well as having perhaps the greater growth potential for future applications.

Some insight into the stability and performance of several nonporous decelerator configurations is provided in the experimental wind-tunnel investigations of references 1 and 2. The scale of the

test models, however, was severely limited by the size of the wind tunnel facilities, thus limiting the usefulness of the data. The degree of decelerator stability reported in these investigations was obtained by observation, a method typical of most wind tunnel tests of towed decelerator systems. Because of the inherent difficulty in obtaining adequate measurements of decelerator stability, emphasis has been placed by some investigators on the use of analytical techniques to determine decelerator stability (references 3 and 4). Though the experimental investigations and analytical studies have illustrated some trends in decelerator dynamics, there still exists a general lack of understanding of the principal factors affecting the dynamic stability of a towed decelerator.

In an effort to shed new light on this problem, a preliminary investigation has been made to determine the geometric and aerodynamic parameters which have the greatest influence on the stability and performance of the nonporous towed decelerator. One of the inherent difficulties arising in this type of study is the variable nature of the geometries of the tow cable and decelerator, both of which are flexible. Also, the towed decelerator is required to operate in the nonuniform flow field aft of the forebody which is being decelerated. As a first step in the analysis of this complex stability problem, several simplifying assumptions are made; the tow cable is assumed to be a rigid rod with a pin connection at each end and the decelerator is assumed to be a rigid body of revolution, the resulting dynamical system being described as a coupled two-body problem. Since the cone

is the basic shape about which other decelerator configurations are designed, specific comments are made concerning this shape during the course of this study. For the present analysis the stability and performance of the towed decelerator are examined for uniform (free stream) flow conditions; such conditions would exist when the wake of the forebody has essentially disappeared, corresponding to a very large tow cable length. Appropriate comments are made to relate the effects of the wake on the stability and performance of the decelerator.

V. LIST OF SYMBOLS

A	aerodynamic axial force on decelerator
A_X, A_Y	reaction forces at attachment point between payload and decelerator system
a_1	length to rod center of gravity, measured along rod axis from origin of rod
a_2	length to decelerator center of gravity, measured along decelerator axis from nose of decelerator
B_X, B_Y	reaction forces at attachment point between rod and decelerator
b_1	length of rod
C_A	axial-force coefficient, $\frac{\text{aerodynamic axial force}}{q_\infty S}$
C_D	drag-force coefficient, $\frac{\text{aerodynamic drag force}}{q_\infty S}$
C_L	lift-force coefficient, $\frac{\text{aerodynamic lift force}}{q_\infty S}$
$C_{L_\alpha} = \frac{\partial C_L}{\partial \alpha}$	lift-force coefficient slope at zero angle of attack
C_m	pitching-moment coefficient, $\frac{\text{aerodynamic pitching moment}}{q_\infty S \bar{c}}$
$C_{m_\alpha} = \frac{\partial C_m}{\partial \alpha}$	pitching-moment coefficient slope at zero angle of attack
C_N	normal-force coefficient, $\frac{\text{aerodynamic normal force}}{q_\infty S}$
$C_{N_\alpha} = \frac{\partial C_N}{\partial \alpha}$	normal-force coefficient slope at zero angle of attack
CG	center of gravity
c	damping term in equivalent spring-mass-dashpot dynamical system

c_{cr}	critical damping representing the limiting case between oscillatory and nonoscillatory motion
$\bar{c}$	reference length of decelerator, taken to be base diameter for conical shapes
D_1	aerodynamic drag force on rod
D_2	aerodynamic drag force on decelerator
g	acceleration due to gravity
h	height of conical decelerator
J	sum of mass moments of inertia of rod and decelerator about the respective centers of gravity of the rod and decelerator
J_1	mass moment of inertia of rod about the center of gravity of the rod
J_2	mass moment of inertia of decelerator about the center of gravity of the decelerator
k	spring constant in equivalent spring-mass-dashpot dynamical system
L_1	aerodynamic lift force on rod
L_2	aerodynamic life force on decelerator
$\frac{\partial L}{\partial \alpha}$	slope of lift-force curve at zero angle of attack
$\frac{\partial L}{\partial \dot{\alpha}}$	rate of change of lift force with rate of change of angle of attack
$\frac{\partial L}{\partial \theta_2}$	rate of change of lift force with pitch angle

$\frac{\partial L}{\partial \dot{\theta}_2}$	rate of change of lift force with pitch velocity
M_1	aerodynamic pitching moment on rod
M_2	aerodynamic pitching moment on decelerator
$\frac{\partial M}{\partial \alpha}$	slope of pitching-moment curve at zero angle of attack
$\frac{\partial M}{\partial \dot{\alpha}}$	rate of change of pitching moment with rate of change of angle of attack
$\frac{\partial M}{\partial \theta_2}$	rate of change of pitching moment with pitch angle
$\frac{\partial M}{\partial \dot{\theta}_2} = \frac{\partial M}{\partial q}$	damping of pitch
m	mass term in equivalent spring-mass-dashpot dynamical system
m_1	mass of rod
m_2	mass of decelerator
N	aerodynamic normal force on decelerator
$\frac{\partial N}{\partial \alpha}$	slope of normal-force curve at zero angle of attack
q	pitch velocity of decelerator, $\dot{\theta}_2$
q_∞	free-stream dynamic pressure
Re	Reynolds number based on decelerator base diameter
Ro	Routh's discriminant
r	radius
r_1 and r_2	roots of governing differential equations of motion describing the transient (or complementary) solutions
S	reference area of decelerator, taken to be the base area for conical shapes

t	time
Δt	time to damp to one-half amplitude
V	cone volume
V_∞	flight speed of payload-decelerator system
v	vertical velocity of decelerator center of gravity
v_1	vertical velocity of nose of decelerator, resulting from rotation about the attachment point between payload and decelerator system
v_2	vertical velocity of center of gravity of decelerator with respect to nose of decelerator, resulting from rotation about the attachment point between rod and decelerator
X, Y	cartesian coordinate system (X axis tangential to flight path)
x_1, y_1	cartesian coordinates of rod center of gravity
x_2, y_2	cartesian coordinates of decelerator center of gravity
α	angle of attack of decelerator center of gravity
β	angle between payload reference axis and horizontal
γ	angle between flight path and horizontal
θ_c	cone semiapex angle
θ_1	angle between rod axis and tangent to flight path
θ_2	angle between decelerator axis and tangent to flight path
θ_{2_i}	induced angle of attack resulting from vertical velocity of the decelerator's center of gravity

θ_{2_p}	particular (steady state) solution of the differential governing equation of motion for decelerator rotating about its nose
ζ	damping factor (ratio of actual damping to critical damping)
ρ	density
ω_d	damped angular frequency
ω_n	natural angular frequency
exp	exponential
ln	natural logarithm
$\sum$	summation
∂	partial derivative
. (dot)	first derivative with respect to time
.. (double dot)	second derivative with respect to time

Subscripts

i	induced angle
l	large
0	initial conditions (time equal zero)
p	particular solution
s	small

VI. THEORETICAL DESCRIPTION OF TOWED DECELERATOR

Mathematical Model

This analysis was performed in order to determine the geometric and aerodynamic parameters having the greatest influence on the stability and performance of the towed decelerator system. In the most general case the dynamics of the towed decelerator are necessarily coupled with the dynamics of the payload, and vice versa, making a straight forward analysis of the decelerator's dynamic characteristics rather difficult. In this investigation, therefore, the angular motion of the payload is assumed zero, so that the problem is simplified and the following analysis can be concentrated on the towed-decelerator dynamics. Since orientation of the flight path does not affect the stability of the decelerator, the decelerator system will be considered in a horizontal mode of operation ($\gamma = 0$ in Figure 1). It should be noted that the most common method of experimentally testing towed decelerators utilizes a payload mounted rigidly in a horizontal position.

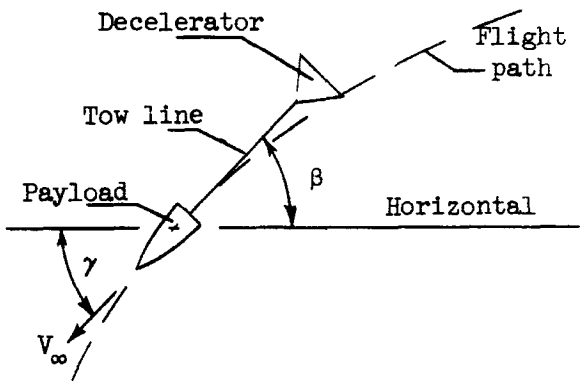

Figure 1.- Schematic of payload-decelerator system.

In reality, the tow line and decelerator are both flexible and represent a multidegree of freedom problem. A general approach to describing this system would be to consider N number of particles

having individual masses. The more restrictive approach of assuming the tow line and decelerator as rigid bodies of revolution is utilized in the present analysis. Only plane motion is considered, yawing and rolling moments being neglected.

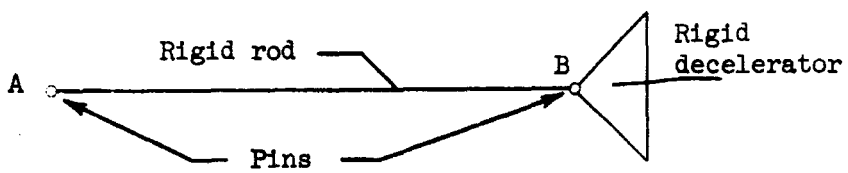

Figure 2.- Two-body system.

The towed decelerator system is illustrated in Figure 2, where pin A represents a fixed pivot point and has no motion, and where pin B is free to rotate with the system. Attachment of the rigid rod and decelerator is at the nose of the decelerator (pin B). This resultant two-body problem is strikingly similar to the double-compound pendulum described by Myklestad in reference 5. The basic differences between the two dynamical systems are: (1) weights in the present analysis represent near constant forcing functions for the system, whereas they act as spring constants in the double-compound pendulum problem, and (2) aerodynamic forces and moment are included in the present analysis. The method of obtaining the differential equations of motion for the present study is identical to that performed by Myklestad. The cartesian coordinate system employed for the two bodies is illustrated in Figure 3, and the

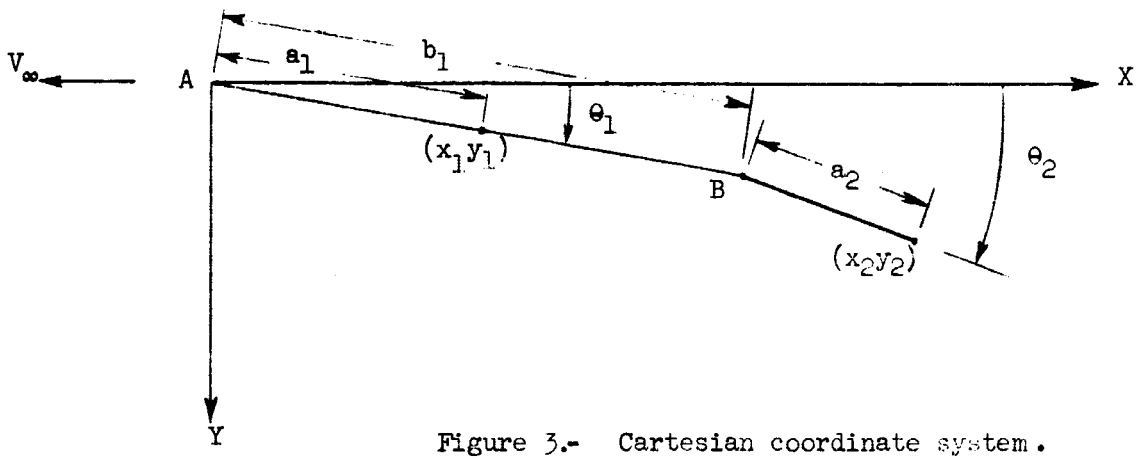

Figure 3.- Cartesian coordinate system.

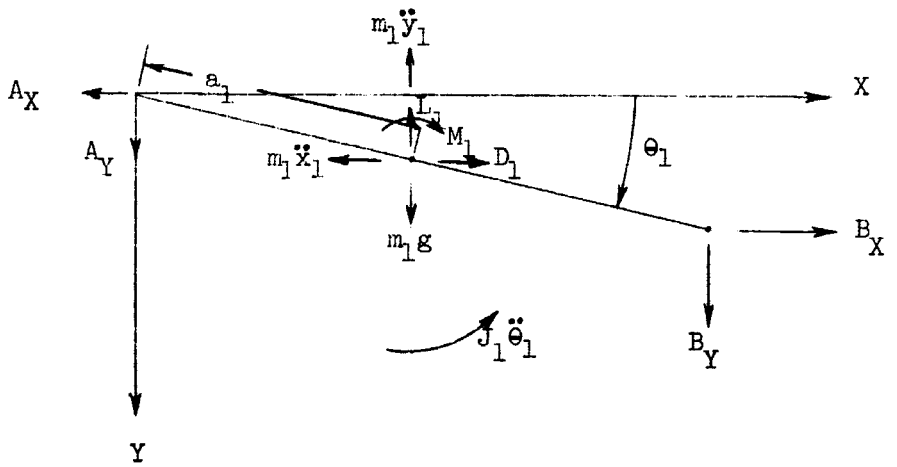

Figure 4.- Free body diagram of rod.

resulting free-body diagrams in Figures 4 and 5. The X-axis is oriented to coincide with the direction of the free-stream velocity vector. The aerodynamic forces and moments of the rod and decelerator are shown in the figures to act at the respective centers of gravity.

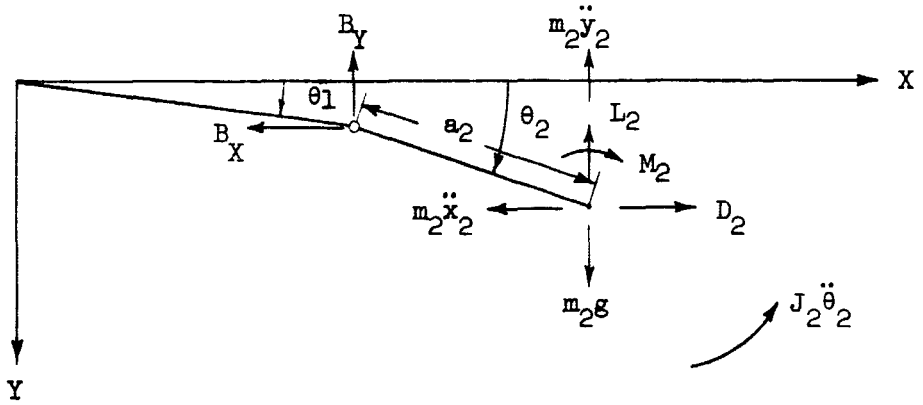

Figure 5.- Free body diagram of decelerator.

In the analysis to follow, the aerodynamic forces and moment on the rod are assumed to be negligible, and likewise the rod's aerodynamic damping.

Equations of Motion

First, the internal reactions B_X and B_Y are found from summing forces in the X and Y directions to be,

$$B_X + m_2 \ddot{x}_2 - D_2 = 0$$

$$B_X = D_2 - m_2 \ddot{x}_2 \tag{1}$$

and

$$B_Y + m_2 \ddot{y}_2 + L_2 - m_2 g = 0$$

$$B_Y = - L_2 - m_2 \ddot{y}_2 + m_2 g \tag{2}$$

Two equations of equilibrium can be obtained from the free-body diagrams by taking moments about pins A and B. Summing moments about A yields

$$\sum M_A = 0 = m_1 g a_1 \cos \theta_1 + m_1 \ddot{x}_1 a_1 \sin \theta_1 - m_1 \ddot{y}_1 a_1 \cos \theta_1 - J_1 \ddot{\theta}_1$$

$$- B_X b_1 \sin \theta_1 + B_Y b_1 \cos \theta_1$$

Substitute for B_X and B_Y from equations (1) and (2) to get

$$\sum M_A = 0 = m_1 g a_1 \cos \theta_1 + m_1 \ddot{x}_1 a_1 \sin \theta_1 - m_1 \ddot{y}_1 a_1 \cos \theta_1 - J_1 \ddot{\theta}_1$$

$$- b_1 D_2 \sin \theta_1 + b_1 \sin \theta_1 \, m_2 \ddot{x}_2 - b_1 \cos \theta_1 \, m_2 \ddot{y}_2$$

$$+ b_1 \cos \theta_1 \left(- L_2 + m_2 g \right) \tag{3}$$

Summing moments about point B yields

$$\sum M_B = 0 = m_2 g a_2 \cos \theta_2 + m_2 \ddot{x}_2 a_2 \sin \theta_2 - m_2 \ddot{y}_2 a_2 \cos \theta_2 - L_2 a_2 \cos \theta_2$$

$$- D_2 a_2 \sin \theta_2 - J_2 \ddot{\theta}_2 + M_2 \tag{4}$$

It is desirable to change the cartesian (CG) coordinates to the generalized coordinates of θ_1 and θ_2. To accomplish this the following relations are used:

$$x_1 = a_1 \cos \theta_1 \qquad x_2 = b_1 \cos \theta_1 + a_2 \cos \theta_2$$

$$y_1 = a_1 \sin \theta_1 \qquad y_2 = b_1 \sin \theta_1 + a_2 \sin \theta_2$$

Differentiating with respect to time yields

$$\dot{x}_1 = - a_1\dot{\theta}_1 \sin \theta_1 \qquad \dot{x}_2 = - b_1\dot{\theta}_1 \sin \theta_1 - a_2\dot{\theta}_2 \sin \theta_2$$

$$\dot{y}_1 = a_1\dot{\theta}_1 \cos \theta_1 \qquad \dot{y}_2 = b_1\dot{\theta}_1 \cos \theta_1 + a_2\dot{\theta}_2 \cos \theta_2$$

$$\ddot{x}_1 = - a_1\ddot{\theta}_1 \sin \theta_1 - a_1\dot{\theta}_1^2 \cos \theta_1 \qquad \ddot{x}_2 = - b_1\ddot{\theta}_1 \sin \theta_1 - b_1\dot{\theta}_1^2 \cos \theta_1 - a_2\ddot{\theta}_2 \sin \theta_2 - a_2\dot{\theta}_2^2 \cos \theta_2$$

$$\ddot{y}_1 = a_1\ddot{\theta}_1 \cos \theta_1 - a_1\dot{\theta}_1^2 \sin \theta_1 \qquad \ddot{y}_2 = b_1\ddot{\theta}_1 \cos \theta_1 - b_1\dot{\theta}_1^2 \sin \theta_1 + a_2\ddot{\theta}_2 \cos \theta_2 - a_2\dot{\theta}_2^2 \sin \theta_2$$

(5)

Substitute the appropriate expressions into equation (5) to get

$$m_1 g a_1 \cos \theta_1 + m_1 a_1 \sin \theta_1 \left(- a_1\ddot{\theta}_1 \sin \theta_1 - a_1\dot{\theta}_1^2 \cos \theta_1\right)$$

$$- m_1 a_1 \cos \theta_1 \left(a_1\ddot{\theta}_1 \cos \theta_1 - a_1\dot{\theta}_1^2 \sin \theta_1\right) - J_1\ddot{\theta}_1$$

$$- b_1 D_2 \sin \theta_1 + b_1 m_2 \sin \theta_1 \left(- b_1 \ddot{\theta}_1 \sin \theta_1 - b_1 \dot{\theta}_1^2 \cos \theta_1 \right.$$

$$\left. - a_2 \ddot{\theta}_2 \sin \theta_2 - a_2 \dot{\theta}_2^2 \cos \theta_2 \right) - b_1 m_2 \cos \theta_1 \left(b_1 \ddot{\theta}_1 \cos \theta_1 \right.$$

$$\left. - b_1 \dot{\theta}_1^2 \sin \theta_1 + a_2 \ddot{\theta}_2 \cos \theta_2 - a_2 \dot{\theta}_2^2 \sin \theta_2 \right)$$

$$+ b_1 \cos \theta_1 \left(- L_2 + m_2 g \right) = 0$$

Assume small displacements so that

$$\sin \theta \approx \theta \quad \text{and} \quad \cos \theta \approx 1$$

Higher order and nonlinear terms such as $\dot{\theta}_1^2$, $\theta_1 \theta_2$, and $\dot{\theta}_2^2$ are neglected; that is, products of the angles and products of their derivatives. Thus,

$$- m_1 g a_1 + m_1 a_1 \left(a_1 \ddot{\theta}_1 \right) + J_1 \ddot{\theta}_1 + b_1 D_2 \theta_1 + b_1 m_2 \left(b_1 \ddot{\theta}_1 + a_2 \ddot{\theta}_2 \right)$$

$$- b_1 \left(- L_2 + m_2 g \right) = 0$$

Collecting terms,

$$\left(m_1 a_1^2 + m_2 b_1^2 + J_1 \right) \ddot{\theta}_1 + b_1 D_2 \theta_1 + a_2 b_1 m_2 \ddot{\theta}_2 + b_1 L_2 = m_1 g a_1 + m_2 g b_1 \tag{6}$$

Substitute expressions (5) into equation (4) to get

$$m_2 g a_2 \cos \theta_2 + m_2 a_2 \sin \theta_2 \left(- b_1 \ddot{\theta}_1 \sin \theta_1 - b_1 \dot{\theta}_1^2 \cos \theta_1 - a_2 \ddot{\theta}_2 \sin \theta_2 \right.$$

$$\left. - a_2 \dot{\theta}_2^2 \cos \theta_2 \right) - m_2 a_2 \cos \theta_2 \left(b_1 \ddot{\theta}_1 \cos \theta_1 - b_1 \dot{\theta}_1^2 \sin \theta_1 \right.$$

$$+ a_2\ddot{\theta}_2 \cos\theta_2 - a_2\dot{\theta}_2^2 \sin\theta_2\Big) - L_2a_2 \cos\theta_2 - D_2a_2 \sin\theta_2$$

$$- J_2\ddot{\theta}_2 + M_2 = 0$$

Again, assume small displacements ($\sin\theta \approx \theta$ and $\cos\theta \approx 1$) and neglect nonlinear terms. There results

$$- m_2ga_2 + m_2a_2\left(b_1\ddot{\theta}_1 + a_2\ddot{\theta}_2\right) + L_2a_2 + D_2a_2\theta_2 + J_2\ddot{\theta}_2 - M_2 = 0$$

Rearranging,

$$m_2a_2b_1\ddot{\theta}_1 + \left(m_2a_2^2 + J_2\right)\ddot{\theta}_2 + D_2a_2\theta_2 + L_2a_2 - M_2 = m_2ga_2 \qquad (7)$$

It is now desirable to consider the aerodynamic forces and moment existing on the decelerator. The reader should note that the subscript 2 associated with the decelerator's aerodynamics will be deleted during the remainder of the discussion.

The angle of attack of the decelerator's center of gravity is defined as follows:

$$\alpha = \theta_2 + \theta_{2_i}$$

where θ_2 represents the angle between the decelerator axis and the X-axis and θ_{2_i} represents the induced angle of attack resulting form vertical velocity of the CG of the decelerator.

Note: The vertical velocity of the decelerator CG consists of two components, v_1 and v_2, resulting from rotation

about pin A and B, respectively (see Figure 6). The component v_2 is the velocity of the decelerator CG with respect to pin B.

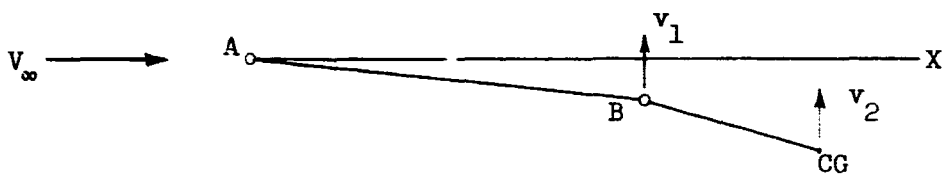

Figure 6.- Induced velocities.

Since small angles of attack are being considered, it follows that

$$\theta_{2_i} = \tan \frac{v}{V_\infty} \approx \frac{v}{V_\infty} = \frac{v_1 + v_2}{V_\infty}$$

It can be seen from Figure 3 that

$$v_1 = b_1\dot{\theta}_1 \quad \text{and} \quad v_2 = a_2\dot{\theta}_2$$

Thus,

$$\theta_{2_i} = \frac{b_1\dot{\theta}_1}{V_\infty} + \frac{a_2\dot{\theta}_2}{V_\infty}$$

The angle of attack of the decelerator is then given by

$$\alpha = \theta_2 + \frac{b_1\dot{\theta}_1}{V_\infty} + \frac{a_2\dot{\theta}_2}{V_\infty} \tag{8}$$

Also,

$$\dot{\alpha} = \dot{\theta}_2 + \frac{b_1\ddot{\theta}_1}{V_\infty} + \frac{a_2\ddot{\theta}_2}{V_\infty}$$

For this analysis the aerodynamic drag force (D) is considered to be independent of angle of attack since $D \sim \alpha^2$. The lift force (L) can be expressed as

$$L = \frac{\partial L}{\partial \alpha}\alpha + \frac{\partial L}{\partial \dot{\alpha}}\dot{\alpha}$$

In keeping with the assumptions of linearization, higher-order terms are not considered. Substituting α and $\dot{\alpha}$ into the expression for lift force,

$$L = \frac{\partial L}{\partial \alpha}\theta_2 + \frac{b_1}{V_\infty}\frac{\partial L}{\partial \alpha}\dot{\theta}_1 + \frac{a_2}{V_\infty}\frac{\partial L}{\partial \alpha}\dot{\theta}_2 + \frac{\partial L}{\partial \dot{\alpha}}\dot{\theta}_2 + \frac{b_1}{V_\infty}\frac{\partial L}{\partial \dot{\alpha}}\ddot{\theta}_1 + \frac{a_2}{V_\infty}\frac{\partial L}{\partial \dot{\alpha}}\ddot{\theta}_2 \tag{9}$$

The aerodynamic pitching moment can be expressed as

$$M = \frac{\partial M}{\partial \alpha}\alpha + \frac{\partial M}{\partial \dot{\alpha}}\dot{\imath} + \frac{\partial M}{\partial \theta_2}\theta_2 + \frac{\partial M}{\partial \dot{\theta}_2}\dot{\theta}_2$$

Substituting for α and $\dot{\alpha}$,

$$M = \frac{\partial M}{\partial \alpha}\theta_2 + \frac{b_1}{V_\infty}\frac{\partial M}{\partial \alpha}\dot{\theta}_1 + \frac{a_2}{V_\infty}\frac{\partial M}{\partial \alpha}\dot{\theta}_2 + \frac{\partial M}{\partial \dot{\alpha}}\dot{\theta}_2 + \frac{b_1}{V_\infty}\frac{\partial M}{\partial \dot{\alpha}}\ddot{\theta}_1 + \frac{a_2}{V_\infty}\frac{\partial M}{\partial \dot{\alpha}}\ddot{\theta}_2 + \frac{\partial M}{\partial \dot{\theta}_2}\dot{\theta}_2 \tag{10}$$

where

$$\frac{\partial M}{\partial \dot{\theta}_2} = \frac{\partial M}{\partial q}$$

Substitute the expression for lift force into equation (6).

$$\left(m_1 a_1^2 + m_2 b_1^2 + J_1\right) \ddot{\theta}_1 + b_1 D\theta_1 + a_2 b_1 m_2 \ddot{\theta}_2 + b_1 \frac{\partial L}{\partial \alpha} \theta_2 + \frac{b_1^2}{V_\infty} \frac{\partial L}{\partial \alpha} \dot{\theta}_1$$

$$+ \frac{a_2 b_1}{V_\infty} \frac{\partial L}{\partial \alpha} \dot{\theta}_2 + b_1 \frac{\partial L}{\partial \dot{\alpha}} \dot{\theta}_2 + \frac{b_1^2}{V_\infty} \frac{\partial L}{\partial \dot{\alpha}} \ddot{\theta}_1 + \frac{a_2 b_1}{V_\infty} \frac{\partial L}{\partial \dot{\alpha}} \ddot{\theta}_2 = m_1 g a_1$$

$$+ m_2 g b_1$$

Collecting terms,

$$\left(m_1 a_1^2 + m_2 b_1^2 + J_1 + \frac{b_1}{V_\infty} \frac{\partial L}{\partial \dot{\alpha}}\right) \ddot{\theta}_1 + \frac{b_1^2}{V_\infty} \frac{\partial L}{\partial \alpha} \dot{\theta}_1 + b_1 D\theta_1 + \left(a_2 b_1 m_2\right.$$

$$\left. + \frac{a_2 b_1}{V_\infty} \frac{\partial L}{\partial \dot{\alpha}}\right) \ddot{\theta}_2 + \left(\frac{a_2 b_1}{V_\infty} \frac{\partial L}{\partial \alpha} + b_1 \frac{\partial L}{\partial \dot{\alpha}}\right) \dot{\theta}_2 + b_1 \frac{\partial L}{\partial \alpha} \theta_2 = m_1 g a_1$$

$$+ m_2 g b_1 \qquad (11)$$

Substitute the expressions for lift force and pitching moment into equation (7).

$$m_2 a_2 b_1 \ddot{\theta}_1 + \left(m_2 a_2^2 + J_2\right) \ddot{\theta}_2 + D a_2 \theta_2 + a_2 \frac{\partial L}{\partial \alpha} \theta_2 + \frac{a_2 b_1}{V_\infty} \frac{\partial L}{\partial \alpha} \dot{\theta}_1$$

$$+ \frac{a_2^2}{V_\infty} \frac{\partial L}{\partial \alpha} \dot{\theta}_2 + a_2 \frac{\partial L}{\partial \dot{\alpha}} \dot{\theta}_2 + \frac{a_2 b_1}{V_\infty} \frac{\partial L}{\partial \dot{\alpha}} \ddot{\theta}_1 + \frac{a_2^2}{V_\infty} \frac{\partial L}{\partial \dot{\alpha}} \ddot{\theta}_2 - \frac{\partial M}{\partial \alpha} \theta_2$$

$$- \frac{b_1}{V_\infty} \frac{\partial M}{\partial \alpha} \dot{\theta}_1 - \frac{a_2}{V_\infty} \frac{\partial M}{\partial \alpha} \dot{\theta}_2 - \frac{\partial M}{\partial \dot{\alpha}} \dot{\theta}_2 - \frac{b_1}{V_\infty} \frac{\partial M}{\partial \dot{\alpha}} \ddot{\theta}_1 - \frac{a_2}{V_\infty} \frac{\partial M}{\partial \dot{\alpha}} \ddot{\theta}_2$$

$$- \frac{\partial M}{\partial q} \dot{\theta}_2 = m_2 g a_2$$

Collecting terms,

$$\left(a_2 b_1 m_2 + \frac{a_2 b_1}{V_\infty}\frac{\partial L}{\partial \dot{\alpha}} - \frac{b_1}{V_\infty}\frac{\partial M}{\partial \dot{\alpha}}\right)\ddot{\theta}_1 + \left(\frac{a_2 b_1}{V_\infty}\frac{\partial L}{\partial \alpha} - \frac{b_1}{V_\infty}\frac{\partial M}{\partial \alpha}\right)\dot{\theta}_1 + \left(m_2 a_2^2 + J_2\right.$$

$$\left. + \frac{a_2^2}{V_\infty}\frac{\partial L}{\partial \dot{\alpha}} - \frac{a_2}{V_\infty}\frac{\partial M}{\partial \dot{\alpha}}\right)\ddot{\theta}_2 + \left(\frac{a_2^2}{V_\infty}\frac{\partial L}{\partial \alpha} + a_2\frac{\partial L}{\partial \dot{\alpha}} - \frac{a_2}{V_\infty}\frac{\partial M}{\partial \alpha} - \frac{\partial M}{\partial \dot{\alpha}} - \frac{\partial M}{\partial q}\right)\dot{\theta}_2$$

$$+ \left(a_2 D + a_2\frac{\partial L}{\partial \alpha} - \frac{\partial M}{\partial \alpha}\right)\theta_2 = m_2 g a_2 \qquad (12)$$

Thus it is seen that equations (11) and (12) represent a system of second order, nonhomogeneous, linear differential equations with constant coefficients.

Before proceeding to the discussion of the possible solutions to these equations, a few comments are necessary concerning the aerodynamic forces and moment assumed to act on the decelerator. As seen in equations (9) and (10) not all of the factors influencing lift force and pitching moment are taken into account. It is believed, however, that the exclusion of these terms will not have an appreciable effect on the results of this analysis. It should be emphasized that the equations of motion apply for any decelerator shape as long as the shape is a body of revolution. One such body of revolution often considered in decelerator problems is the conical shape (this shape forms the basis for most decelerator designs). Experimental data obtained on a series of cone bodies at free-stream conditions (reference 6) are shown in Figure 7 and illustrate the linear nature of lift force and pitching moment with angle of attack; also, drag force is approximately constant at angles of attack near

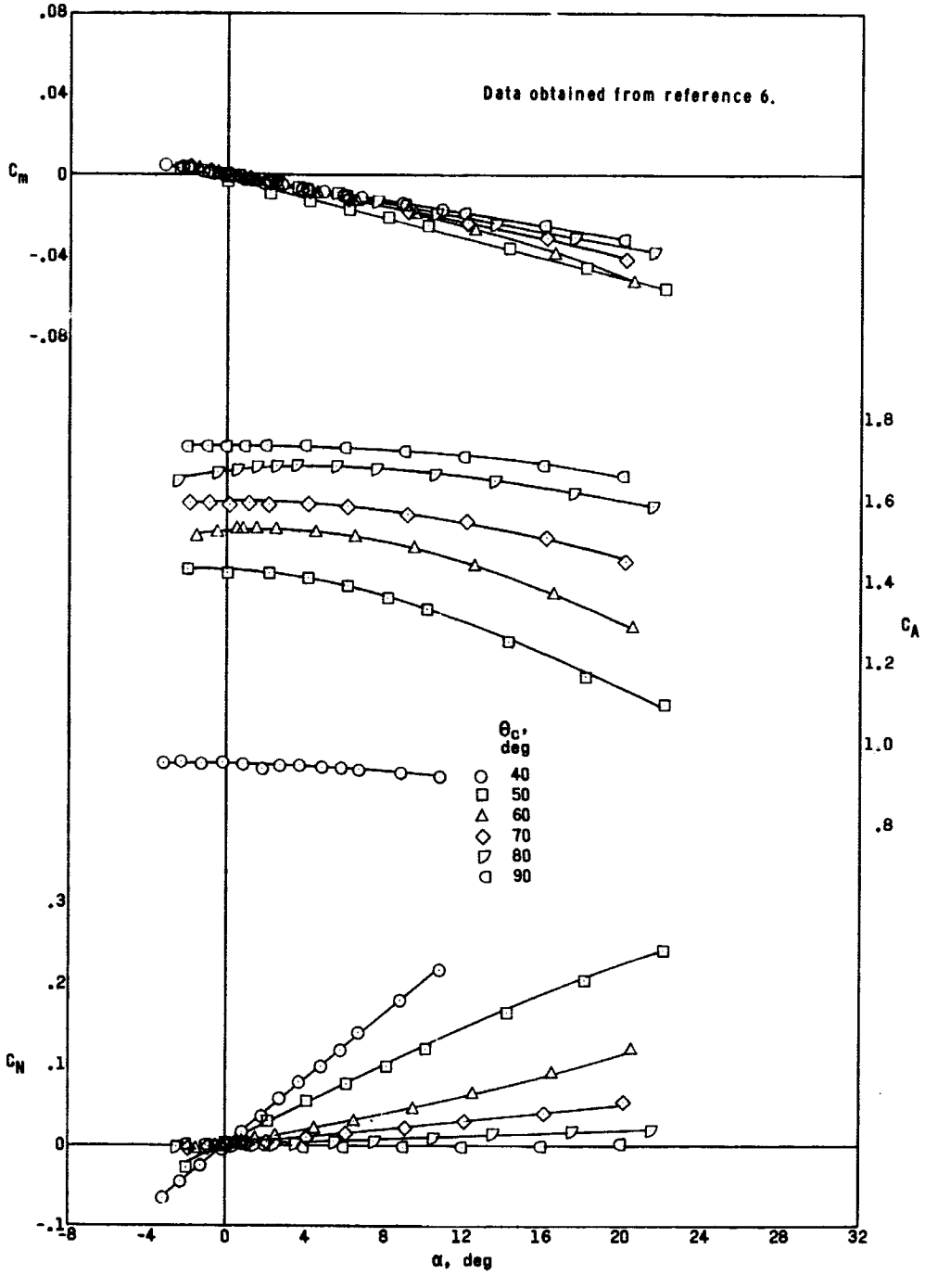

(a) Body axis.

Figure 7.- Variation of longitudinal characteristics with angle of attack for family of cone models; M = 4.63, Re = 0.8×10^6.

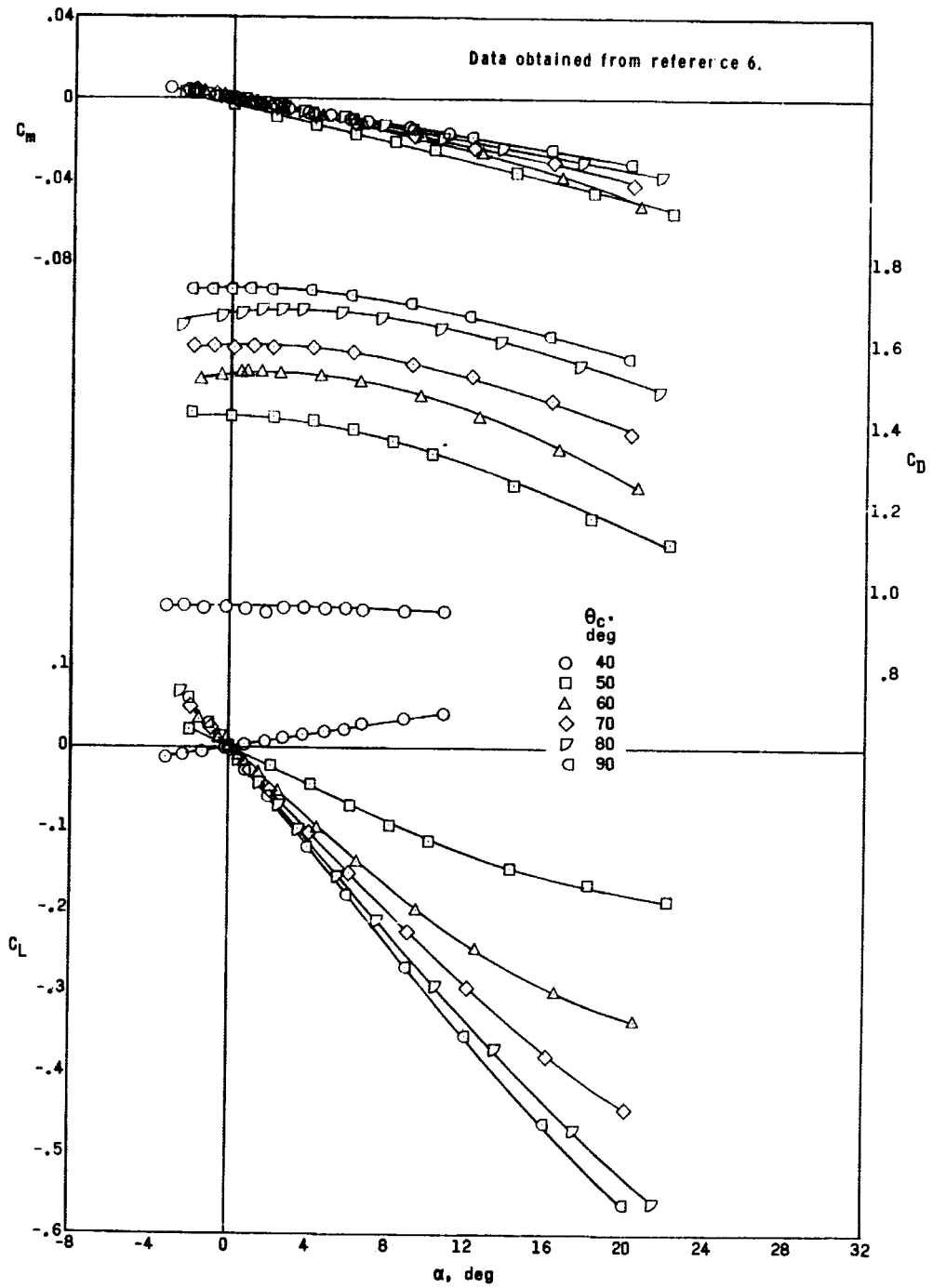

(b) Stability axis.

Figure 7.- Concluded.

zero since $D \sim \alpha^2$. Such conditions would exist on a towed conical decelerator when the wake of the forebody has essentially disappeared, corresponding to a very large tow cable length (b_1). The question arises, however, of how the aerodynamic forces and moment vary with angle of attack if the cone is subjected to the nonuniform flow field associated with the wake. The answer to this question appears formidable at the present time because of the dependence of the aerodynamics on the size of the cone (with respect to the forebody), the location of the cone in the wake, forebody geometry, free-stream Mach number and Reynolds number, boundary-layer buildup and separation effects on the tow cable, and on cone semiapex angle. The possibility exists that to adequately describe the aerodynamics of the cone in a nonuniform flow field, it may be necessary to retain higher order terms, thus defeating the simplicity of the approach of the present analysis. For these reasons, free-stream flow conditions are assumed to exist. The reader should note that the following analysis, though concerned principally with the conical shaped decelerator, could be applied equally well to any shape body for which the geometric and aerodynamic parameters are known.

Two-Body Problem

To evaluate the system of second-order differential equations, the terms involving $\frac{\partial L}{\partial \dot{\alpha}}$ and $\frac{\partial M}{\partial \dot{\alpha}}$ are assumed to be negligible; this has been

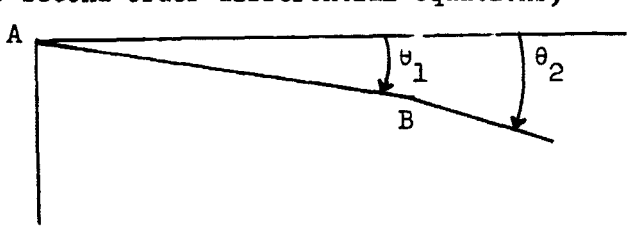

shown in the stability investigation of reference 7 to be a justifiable assumption at high Mach numbers. Equations (11) and (12) therefore reduce to

$$\left(m_1 a_1^2 + m_2 b_1^2 + J_1\right) \ddot{\theta}_1 + \frac{b_1^2}{V_\infty} \frac{\partial L}{\partial \alpha} \dot{\theta}_1 + b_1 D\theta_1 + \left(a_2 b_1 m_2\right) \ddot{\theta}_2$$

$$+ \left(\frac{a_2 b_1}{V_\infty} \frac{\partial L}{\partial \alpha}\right) \dot{\theta}_2 + b_1 \frac{\partial L}{\partial \alpha} \theta_2 = m_1 g a_1 + m_2 g b_1 \tag{13}$$

and

$$\left(a_2 b_1 m_2\right) \ddot{\theta}_1 + \left(\frac{a_2 b_1}{V_\infty} \frac{\partial L}{\partial \alpha} - \frac{b_1}{V_\infty} \frac{\partial M}{\partial \alpha}\right) \dot{\theta}_1 + \left(m_2 a_2^2 + J_2\right) \ddot{\theta}_2 + \left(\frac{a_2^2}{V_\infty} \frac{\partial L}{\partial \alpha}\right.$$

$$\left. - \frac{a_2}{V_\infty} \frac{\partial M}{\partial \alpha} - \frac{\partial M}{\partial q}\right) \dot{\theta}_2 + \left(a_2 D + a_2 \frac{\partial L}{\partial \alpha} - \frac{\partial M}{\partial \alpha}\right) \theta_2 = m_2 g a_2 \tag{14}$$

Characteristic equation.- To arrive at a characteristic equation representing the system described by equations (13) and (14) it is beneficial to write these equations as

$$\begin{aligned} A \ddot{\theta}_1 + B \dot{\theta}_1 + C \theta_1 + D \ddot{\theta}_2 + E \dot{\theta}_2 + F \theta_2 &= G \\ H \ddot{\theta}_1 + I \dot{\theta}_1 + J \ddot{\theta}_2 + K \dot{\theta}_2 + L \theta_2 &= M \end{aligned} \tag{15}$$

where

$$A = m_1 a_1^2 + m_2 b_1^2 + J_1 \qquad E = \frac{a_2 b_1}{V_\infty} \frac{\partial L}{\partial \alpha}$$

$$B = \frac{b_1}{V_\infty} \frac{\partial L}{\partial \alpha} \qquad F = b_1 \frac{\partial L}{\partial \alpha}$$

$$C = b_1 D$$

$$G = m_1 g a_1 + m_2 g b_1$$

$$D = a_2 b_1 m_2$$

$$H = a_2 b_1 m_2 \qquad K = \frac{a_2^2}{V_\infty}\frac{\partial L}{\partial \alpha} - \frac{a_2}{V_\infty}\frac{\partial M}{\partial \alpha} - \frac{\partial M}{\partial q}$$

$$I = \frac{a_2 b_1}{V_\infty}\frac{\partial L}{\partial \alpha} - \frac{b_1}{V_\infty}\frac{\partial M}{\partial \alpha} \qquad L = a_2\left(\frac{\partial L}{\partial \alpha} + D\right) - \frac{\partial M}{\partial \alpha}$$

$$J = m_2 a_2^2 + J_2 \qquad M = m_2 g a_2$$

Consider the homogeneous case.

$$A\,\ddot{\theta}_1 + B\,\dot{\theta}_1 + C\,\theta_1 + D\,\ddot{\theta}_2 + E\,\dot{\theta}_2 + F\,\theta_2 = 0$$

$$H\,\ddot{\theta}_1 + I\,\dot{\theta}_1 + J\,\ddot{\theta}_2 + K\,\dot{\theta}_2 + L\,\theta_2 = 0$$

Assume solutions of the form

$$\theta_1 = \tilde{\theta}_1\, e^{\lambda t} \quad \text{and} \quad \theta_2 = \tilde{\theta}_2\, e^{\lambda t}$$

so that

$$\dot{\theta}_1 = \lambda\,\tilde{\theta}_1\, e^{\lambda t} \qquad \dot{\theta}_2 = \lambda\,\tilde{\theta}_2\, e^{\lambda t}$$

$$\ddot{\theta}_1 = \lambda^2\,\tilde{\theta}_1\, e^{\lambda t} \qquad \ddot{\theta}_2 = \lambda^2\,\tilde{\theta}_2\, e^{\lambda t}$$

Substitute and divide by $e^{\lambda t}$ to get

$$\begin{aligned} A\lambda^2\tilde{\theta}_1 + B\lambda\tilde{\theta}_1 + C\tilde{\theta}_1 + D\lambda^2\tilde{\theta}_2 + E\lambda\tilde{\theta}_2 + F\tilde{\theta}_2 &= 0 \\ H\lambda^2\tilde{\theta}_1 + I\lambda\tilde{\theta}_1 + J\lambda^2\tilde{\theta}_2 + K\lambda\tilde{\theta}_2 + L\tilde{\theta}_2 &= 0 \end{aligned} \tag{16}$$

Collecting terms,

$$\left(A\lambda^2 + B\lambda + C\right)\tilde{\theta}_1 + \left(D\lambda^2 + E\lambda + F\right)\tilde{\theta}_2 = 0$$

$$\left(H\lambda^2 + I\lambda\right)\tilde{\theta}_1 + \left(J\lambda^2 + K\lambda + L\right)\tilde{\theta}_2 = 0$$

These are algebraic, homogeneous, linear equations for the constants $\tilde{\theta}_1$ and $\tilde{\theta}_2$. They always have at least the trivial soltuion $\tilde{\theta}_1 = \tilde{\theta}_2 = 0$, which corresponds to $\theta_1 = \theta_2 = 0$. These equations have a nontrivial solution precisely when the determinant of the coefficients is zero.

$$\begin{vmatrix} \left(A\lambda^2 + B\lambda + C\right) & \left(D\lambda^2 + E\lambda + F\right) \\ \left(H\lambda^2 + I\lambda\right) & \left(J\lambda^2 + K\lambda + L\right) \end{vmatrix} = 0$$

Expanding this determinant and collecting terms yields the characteristic equation,

$$(AJ - HD)\,\lambda^4 + (AK + BJ - HE - ID)\,\lambda^3 + (AL + BK + CJ - HF - IE)\,\lambda^2 + (BL + CK - IF)\,\lambda + CL = 0 \qquad (17)$$

Numerical constants could be introduced and exact roots found from this equation, but for the purpose of defining stability it is necessary to look only at the signs which these constants carry.

Stability criteria.- The necessary and sufficient condition for the stability of the dynamic system represented by the quartic,

$$A' \lambda^4 + B' \lambda^3 + C' \lambda^2 + D' \lambda + E' = 0$$

is that

$$A', B', C', D', \text{ and } E' > 0$$

and

$$R_o = B'C'D' - B'^2E' - A'D'^2 > 0$$

This latter grouping of constants is known as Routh's discriminant. It is first necessary to evaluate the coefficients of the quartic, equation (17), and to see under what conditions they might change signs.

$$A' \equiv AJ - HD = \left(m_1 a_1^2 + m_2 b_1^2 + J_1\right)\left(m_2 a_2^2 + J_2\right) - a_2 b_1 m_2 \left(a_2 b_1 m_2\right)$$

$$= m_1 m_2 a_1^2 + m_2 a_2^2 J_1 + J_2\left(m_1 a_1^2 + m_2 b_1^2 + J_1\right)$$

Thus, this coefficient is positive for all combinations of masses, mass moments of inertia, tow line lengths, and center of gravity locations.

$$B' \equiv AK + BJ - HE - ID = \left(m_1 a_1^2 + m_2 b_1^2 + J_1\right)\left(\frac{a_2^2}{V_\infty}\frac{\partial L}{\partial \alpha} - \frac{a_2}{V_\infty}\frac{\partial M}{\partial \alpha} - \frac{\partial M}{\partial q}\right)$$

$$+ \frac{b_1^2}{V_\infty}\frac{\partial L}{\partial \alpha}\left(m_2 a_2^2 + J_2\right) - a_2 b_1 m_2\left(\frac{a_2 b_1}{V_\infty}\frac{\partial L}{\partial \alpha}\right) - \left(\frac{a_2 b_1}{V_\infty}\frac{\partial L}{\partial \alpha} - \frac{b_1}{V_\infty}\frac{\partial M}{\partial \alpha}\right) a_2 b_1 m_2$$

Expanding,

$$B' = \left(m_1 a_1^2 a_2^2 + J_1 a_2^2 + J_2 b_1^2\right) \frac{1}{V_\infty} \frac{\partial L}{\partial \alpha} - \left(m_1 a_1^2 a_2 + J_1 a_2\right) \frac{1}{V_\infty} \frac{\partial M}{\partial \alpha}$$

$$- \left(m_1 a_1^2 + m_2 b_1^2 + J_1\right) \frac{\partial M}{\partial q}$$

Since for bodies of revolution (such as the cone) $\frac{\partial M}{\partial \alpha}$ and $\frac{\partial M}{\partial q}$ are usually negative, B' is definitely positive when $\frac{\partial L}{\partial \alpha} \geq 0$. When B' = 0, the lift-curve slope is of negative value and is given by the expression

$$\left(m_1 a_1^2 a_2^2 + J_1 a_2^2 + J_2 b_1^2\right) \frac{\partial L}{\partial \alpha} = \left(m_1 a_1^2 a_2 + J_1 a_2\right) \frac{\partial M}{\partial \alpha}$$

$$+ V_\infty \left(m_1 a_1^2 + m_2 b_1^2 + J_1\right) \frac{\partial M}{\partial q} \qquad (18)$$

Also,

$$C' \equiv AL + BK + CJ - HF - IE = \left(m_1 a_1^2 + m_2 b_1^2 + J_1\right) \left[a_2 \left(\frac{\partial L}{\partial \alpha} + D\right) - \frac{\partial M}{\partial \alpha}\right]$$

$$+ \frac{b_1^2}{V_\infty} \frac{\partial L}{\partial \alpha} \left[\frac{a_2^2}{V_\infty} \frac{\partial L}{\partial \alpha} - \frac{a_2}{V_\infty} \frac{\partial M}{\partial \alpha} - \frac{\partial M}{\partial q}\right] + b_1 D\left(m_2 a_2^2 + J_2\right) - a_2 b_1^2 m_2 \frac{\partial L}{\partial \alpha}$$

$$- \frac{a_2 b_1}{V_\infty} \frac{\partial L}{\partial \alpha} \left(\frac{a_2 b_1}{V_\infty} \frac{\partial L}{\partial \alpha} - \frac{b_1}{V_\infty} \frac{\partial M}{\partial \alpha}\right)$$

Expanding this expression and at the same time noting that $\frac{\partial N}{\partial \alpha} = \frac{\partial L}{\partial \alpha} + D$ (see subsequent discussion on page 42), it can be shown that

$$C' = m_1 a_1^2 a_2 \frac{\partial N}{\partial \alpha} + m_2 a_2 b_1^2 D + a_2 J_1 \frac{\partial N}{\partial \alpha} + b_1 D\left(m_2 a_2^2 + J_2\right) - \frac{b_1^2}{V_\infty} \frac{\partial L}{\partial \alpha} \frac{\partial M}{\partial q}$$

$$- \frac{\partial M}{\partial \alpha} \left(m_1 a_1^2 + m_2 b_1^2 + J_1\right)$$

As seen in Figure 7 for conical bodies, $\frac{\partial N}{\partial \alpha}$ is always greater than zero. Thus, when $\frac{\partial L}{\partial \alpha} \geq 0$, this coefficient is definitely positive. When $\frac{\partial L}{\partial \alpha} < 0$, C' is probably positive since the negative term involving $\frac{\partial L}{\partial \alpha}$ would be outweighted by the other positive terms.

Now,

$$D' \equiv BL + CK - IF = \frac{b_1^2}{V_\infty} \frac{\partial L}{\partial \alpha} \left[a_2 \left(\frac{\partial L}{\partial \alpha} + D \right) - \frac{\partial M}{\partial \alpha} \right] + b_1 D \left(\frac{a_2^2}{V_\infty} \frac{\partial L}{\partial \alpha} \right.$$

$$\left. - \frac{a_2}{V_\infty} \frac{\partial M}{\partial \alpha} - \frac{\partial M}{\partial q} \right) - b_1 \frac{\partial L}{\partial \alpha} \left(\frac{a_2 b_1}{V_\infty} \frac{\partial L}{\partial \alpha} - \frac{b_1}{V_\infty} \frac{\partial M}{\partial \alpha} \right)$$

which expands to give

$$D' = \left(a_2 b_1^2 + a_2^2 b_1 \right) \frac{D}{V_\infty} \frac{\partial L}{\partial \alpha} - \frac{a_2 b_1}{V_\infty} D \frac{\partial M}{\partial \alpha} - b_1 D \frac{\partial M}{\partial q}$$

When the lift-curve slope is greater than zero, the coefficient D' is definitely greater than zero. When D' = 0, the lift-curve slope is of negative value and is expressed as

$$\frac{\partial L}{\partial \alpha} = \frac{1}{(a_2 + b_1)} \frac{\partial M}{\partial \alpha} + \frac{V_\infty}{a_2 (a_2 + b_1)} \frac{\partial M}{\partial q} \tag{19}$$

Lastly,

$$E' \equiv CL = b_1 D \left[a_2 \left(\frac{\partial L}{\partial \alpha} + D \right) - \frac{\partial M}{\partial \alpha} \right]$$

$$= b_1 D \left(a_2 \frac{\partial N}{\partial \alpha} - \frac{\partial M}{\partial \alpha} \right)$$

Thus, this coefficient is always positive.

It has been mentioned that it is a necessary condition for the coefficients of the stability quartic to be positive valued to ensure a stable dynamical system. If any of the coefficients, say B' and/or D', were to become negative, then the dynamical system is unquestionably unstable. This has been shown to be the case when the lift-curve slope has a negative value less than that expressed by equations (18) and (19). Some support for this argument in the form of experimental data has been published in reference 1. These data indicate that towed cones with semiapex angles up to 40° are definitely stable, 45° cones being marginly stable, and cones with larger semiapex angles being unstable. The major change in any of the aerodynamic parameters between a 40° cone and a 50° cone is the change in sign of the lift curve slope (see Figure 7), $\frac{\partial L}{\partial \alpha}$ being > 0 for the 40° cone and $\frac{\partial L}{\partial \alpha}$ being < 0 for the 50° cone.

To show definitely that the quartic, expressed in equation (17), represents a stable system it is necessary to analyze Routh's discriminant,

$$R_o = B'C'D' - B'^2E' - A'D'^2$$

However, manipulation of the coefficients to provide a general expression for Routh's discriminant without making any simplying assumptions or without substitution of numerical values is extremely tedious. Though evaluation of this discriminant is left to future investigations, it is believed that Routh's discriminant will be greater than zero if the lift-curve slope is greater than zero.

Descartes' Rule of Signs.- To determine the number of real roots existing for the quartic, equation (17), Descartes' Rule of Signs is used and is stated as follows:

> A polynomial equation, $f(x) = 0$, with real coefficients and arranged in descending powers of x, can have no more positive real roots than there are variations of sign between successive terms in $f(x)$, and can have no more negative real roots than there are variations of sign between successive terms in $f(-x)$.
>
> (reference 8)

As has been shown, the quartic of equation (17) may be written as

$$A'\lambda^4 + B'\lambda^3 + C'\lambda^2 + D'\lambda + E' = 0 \qquad (20)$$

where A', B', C', D', and E' are real coefficients and are equal to those constants shown in equation (17). If $\frac{\partial L}{\partial \alpha} \geq 0$, it has been shown that all the coefficients in equation (20) are positive,

$$A',B',C',D',E' > 0$$

Applying Descartes' Rule of Signs it is seen that for $f(\lambda)$ all the coefficients are positive so that there is no variation of sign. Thus, there can be no positive real roots. For $f(-\lambda)$, equation (20) becomes

$$A'\lambda^4 - B'\lambda^3 + C'\lambda^2 - D'\lambda + E' = 0$$

showing that there are four (4) variations of sign. Therefore, there can be up to four negative real roots. Since there are no positive real roots, there will be either zero, two, or four negative real roots.

If $\frac{\partial L}{\partial \alpha} < 0$, it has been shown previously that $A',C',E' > 0$ and B' and D' can be less than zero. Letting $B' = -B''$ and

$D' = - D''$ in equation (20),

$$A'\lambda^4 - B''\lambda^3 + C'\lambda^2 - D''\lambda + E' = 0 \qquad (21)$$

Applying Descartes' Rule of Signs it is seen that for $f(\lambda)$ there are four (4) variations of sign indicating that the quartic can have no more than four positive real roots. For $f(-\lambda)$, equation (21) becomes

$$A'\lambda^4 + B''\lambda^3 + C'\lambda^2 + D''\lambda + E' = 0$$

showing that there are no variation of sign. Therefore, there can be no negative real roots. Thus, if any real roots exist, they will be positive indicating instability.

Review of Solutions to Second-Order Differential Equations and Stability Criteria

It is now desirable to consider two particular cases of single degree of freedom. These two special cases are (1) motion of the decelerator about its nose (pin B) with $\theta_1 = 0^\circ$, and (2) motion of the rod and decelerator about the pivot point (pin A) with $\theta_2 = \theta_1$. Since both of these special cases are represented by a second-order differential equation, it may be beneficial for the reader to review the types of transient motions possible with this type of equation.

The equivalent spring-mass-dashpot dynamical system is described by the equation of motion,

$$m\ddot{\theta} + c\dot{\theta} + k\theta = 0 \qquad (22)$$

the roots of which are given by

$$r_{1,2} = -\frac{c}{2m} \pm \sqrt{\frac{c^2}{4m^2} - \frac{k}{m}} \quad \text{where} \quad \theta = A_1 e^{r_1 t} + A_2 e^{r_2 t}$$

The limiting case between oscillatory and nonoscillatory motions is when the radical equals zero. The value of damping for this condition is called <u>critical damping</u>, c_{cr}.

$$c_{cr}^2 = 4mk \quad \text{or} \quad c_{cr} = 2\sqrt{mk}$$

and since

$$\omega_n = \sqrt{\frac{k}{m}}, \quad \text{then} \quad c_{cr} = 2m\omega_n \ .$$

The dimensionless ratio c/c_{cr} is called the <u>damping factor</u>, ξ.

$$\xi = \frac{c}{c_{cr}} = \frac{c}{2\sqrt{km}} = \frac{c}{2m\omega_n} = \frac{\text{actual damping}}{\text{critical damping}}$$

Using these definitions, the original equation (22) can be written in the form

$$\ddot{\theta} + 2\xi\omega_n\dot{\theta} + \omega_n^2\theta = 0 \qquad (23)$$

where the roots are now given by

$$r_{1,2} = -\xi\omega_n \pm \omega_n\sqrt{\xi^2 - 1}$$

It is seen that the roots are:

(a) real if $\xi > 1$; the motion is overdamped and the transient solution is defined by two exponential terms

(b) equal if $\xi = 1$; the actual damping is equal to the critical damping

(c) complex if $\xi < 1$; the motion is underdamped and the transient solution is oscillatory

(d) imaginary if $\xi = 0$; oscillates at natural frequency with no damping.

As a consequence, $\xi = 1$ separates the regions of motion (see Figure 8).

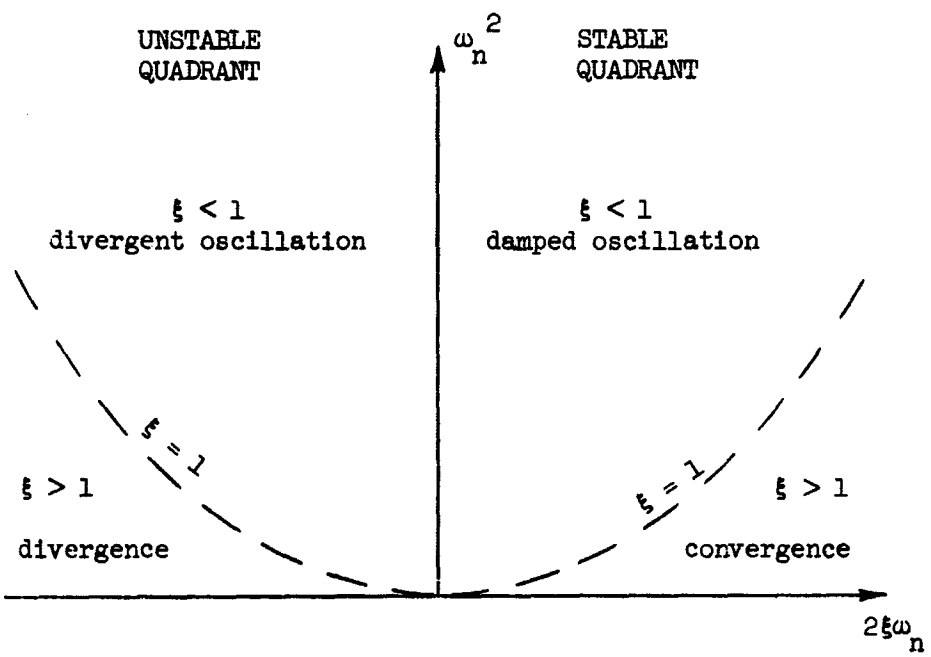

Figure 8.- Regions of motion.

This figure also illustrates one of the basic characteristics of a dynamical system: the motion can be classed as stable provided the coefficients of the governing equation of motion (23) are greater than

zero. Thus,

$$2\xi\,\omega_n \equiv \frac{c}{m} > 0 \quad \text{and} \quad \omega_n^2 \equiv \frac{k}{m} > 0$$

This simply states that the damping and spring constants have to be positive valued to insure a stable system. For a more detailed review of the transient solutions of second-order differential equations and the resulting stability criteria, the reader is referred to references 5 and 8.

Now that the types of transient motions possible for a dynamical system have been reviewed, the special case of the motion of the decelerator about its nose (pin B) will be considered.

Motion of Decelerator About Its Nose - Special Case No. 1

Using equation (14) and letting $\theta_1 = \dot{\theta}_1 = \ddot{\theta}_1 = 0$, the equation of motion of the decelerator about its nose (pin B) can be shown to be

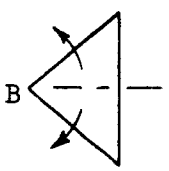

$$\left(m_2 a_2^2 + J_2\right)\ddot{\theta}_2 + \left(\frac{a_2^2}{V_\infty}\frac{\partial L}{\partial \alpha} - \frac{a_2}{V_\infty}\frac{\partial M}{\partial \alpha} - \frac{\partial M}{\partial q}\right)\dot{\theta}_2 + \left[a_2\left(\frac{\partial L}{\partial \alpha} + D\right) - \frac{\partial M}{\partial \alpha}\right]\theta_2 = m_2 g a_2 \tag{24}$$

Looking first at the nonhomogeneous condition, from equation (24) it is seen that

$$\left(m_2 a_2^2 + J_2\right)\ddot{\theta}_{2_p} + \left(\frac{a_2^2}{V_\infty}\frac{\partial L}{\partial \alpha} - \frac{a_2}{V_\infty}\frac{\partial M}{\partial \alpha} - \frac{\partial M}{\partial q}\right)\dot{\theta}_{2_p} + \left[a_2\left(\frac{\partial L}{\partial \alpha} + D\right) - \frac{\partial M}{\partial \alpha}\right]\theta_{2_p} = m_2 g a_2$$

Assume a solution to match the right side of this equation.

$$\theta_{2_p} = \text{constant}$$

Therefore,

$$\dot{\theta}_{2_p} = \ddot{\theta}_{2_p} = 0$$

and

$$\left[a_2\left(\frac{\partial L}{\partial \alpha} + D\right) - \frac{\partial M}{\partial \alpha}\right] \theta_{2_p} = m_2 g a_2$$

The particular solution for equation (24), giving the equilibrium position of the cone, is thus

$$\theta_{2_p} = \frac{m_2 g a_2}{\left[a_2\left(\frac{\partial L}{\partial \alpha} + D\right) - \frac{\partial M}{\partial \alpha}\right]} \tag{25}$$

The homogeneous condition of equation (24) is seen to be

$$\left(m_2 a_2^{\,2} + J_2\right)\ddot{\theta}_2 + \left(\frac{a_2^{\,2}}{V_\infty}\frac{\partial L}{\partial \alpha} - \frac{a_2}{V_\infty}\frac{\partial M}{\partial \alpha} - \frac{\partial M}{\partial q}\right)\dot{\theta}_2 + \left[a_2\left(\frac{\partial L}{\partial \alpha} + D\right) - \frac{\partial M}{\partial \alpha}\right]\theta_2 = 0 \tag{26}$$

This is in the same form as equations (22) and (23) in the review, where

$$\omega_n = \sqrt{\frac{k}{m}} = \sqrt{\frac{a_2\left(\frac{\partial L}{\partial \alpha} + D\right) - \frac{\partial M}{\partial \alpha}}{m_2 a_2^{\,2} + J_2}}$$

and

$$\xi = 2\frac{c}{\sqrt{km}} = 2\frac{\frac{a_2^{\,2}}{V_\infty}\frac{\partial L}{\partial \alpha} - \frac{a_2}{V_\infty}\frac{\partial M}{\partial \alpha} - \frac{\partial M}{\partial q}}{\sqrt{\left(m_2 a_2^{\,2} + J_2\right)\left[a_2\left(\frac{\partial L}{\partial \alpha} + D\right) - \frac{\partial M}{\partial \alpha}\right]}}$$

As pointed out in the review of solutions to second-order differential equations, the types of roots depend on the value of the damping factor, ξ. The transient (or complementary) solutions associated with the homogeneous equation, (26), for various values of damping factor are derived in the following discussion and are added to the particular solution, equation (25), to obtain the complete solution of equation (24).

$\xi > 1$.- The transient solution of equation (26) for $\xi > 1$ is

$$\theta_2 = A\, e^{r_1 t} + B\, e^{r_2 t}$$

where

$$r_1 = -\xi\,\omega_n + \omega_n\sqrt{\xi^2 - 1} \quad \text{and} \quad r_2 = -\xi\,\omega_n - \omega_n\sqrt{\xi^2 - 1}$$

The transient solution can be written as

$$\theta_2 = A \exp\left(-\xi\,\omega_n + \omega_n\sqrt{\xi^2 - 1}\right) t + B \exp\left(-\xi\,\omega_n - \omega_n\sqrt{\xi^2 - 1}\right) t$$

or

$$\theta_2 = e^{-\xi\omega_n t}\left[A \exp\left(\sqrt{\xi^2 - 1}\,\omega_n t\right) + B \exp\left(-\sqrt{\xi^2 - 1}\,\omega_n t\right)\right] \quad (27)$$

Combining equations (25) and (27), the complete solution of equation (24) for $\xi > 1$ is seen to be

$$\theta_2 = e^{-\xi\omega_n t}\left[A \exp\left(\sqrt{\xi^2 - 1}\,\omega_n t\right) + B \exp\left(-\sqrt{\xi^2 - 1}\,\omega_n t\right)\right] + \theta_{2_p} \quad (28)$$

where the constants A and B are determined by initial conditions.

The motion of θ_2 as a function of the dimensionless parameter $\omega_n t$ is shown in Figure 9 for several values of damping factor. As would be expected, the motion is an exponential function of time, the

more sluggish motion occuring for the larger damping factor. To obtain the solution for $\xi = 1$ it is necessary to again utilize equation (26).

$\xi = 1$.- The roots of the characteristic equation are

$$r_1 = r_2 = -\omega_n$$

so that the solution is

$$\theta_2 = A\, e^{-\omega_n t} + Bt\, e^{-\omega_n t} \tag{29}$$

Combining this with equation (25), the complete solution of equation (24) for $\xi = 1$ is

$$\theta_2 = (A + Bt)\, e^{-\omega_n t} + \theta_{2_p} \tag{30}$$

Note that $\theta_2 \rightarrow \theta_{2_p}$ as $t \rightarrow \infty$. This is the expression used to illustrate the motion of θ_2 with $\omega_n t$ in Figure 9 for $\xi = 1$.

$\xi < 1$.- The type of dynamical motion occuring more often than not in aerodynamic stability problems is that which is oscillatory in nature, having a value of actual damping less than the critical damping ($\xi < 1$). In this case the roots of the characteristic equation are complex and are written as

$$r_1 = -\xi\,\omega_n + i\omega_n\sqrt{1 - \xi^2} \quad \text{and} \quad r_2 = -\xi\,\omega_n - i\omega_n\sqrt{1 - \xi^2}$$

The solution of the homogeneous equation (26) is thus,

$$\theta_2 = e^{-\xi\omega_n t}\left(A \cos\sqrt{1 - \xi^2}\,\omega_n t + B \sin\sqrt{1 - \xi^2}\,\omega_n t\right) \tag{31}$$

where $\omega_d = \omega_n\sqrt{1 - \xi^2}$ is the damped frequency of the motion.

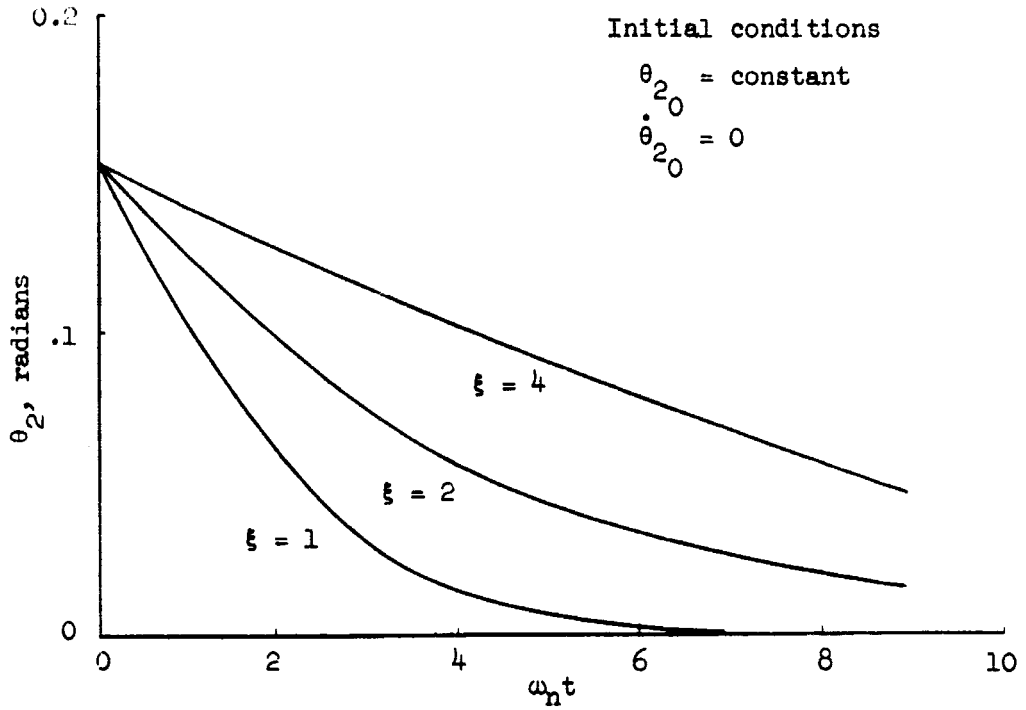

Figure 9.- Effect of damping factor on aperiodic motion.

Equations (28) and (30)

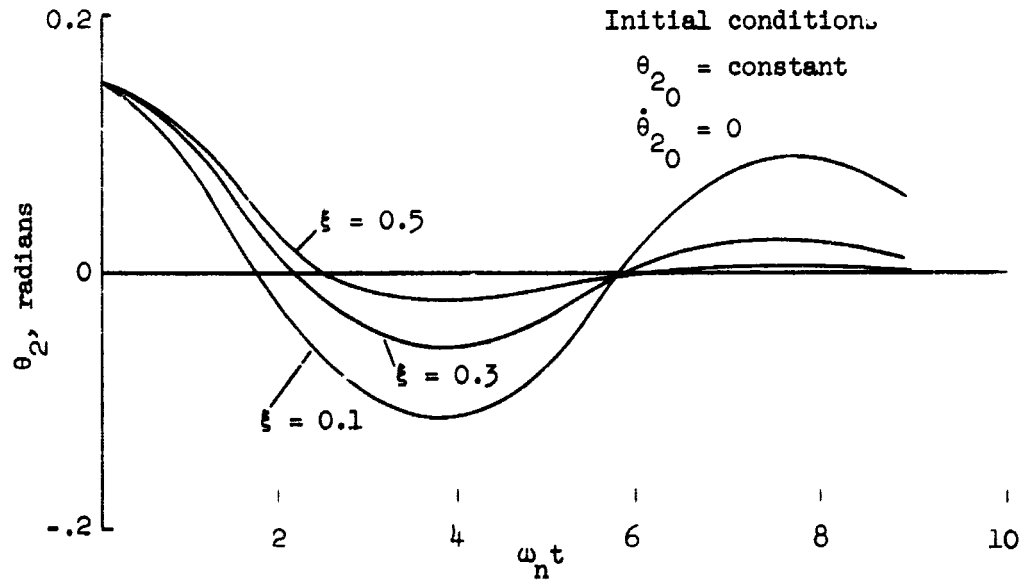

Figure 10.- Effect of damping factor on oscillatory motion.

Equation (32)

Combining this transient solution with the particular solution, equation (25), yields the complete solution of equation (24) for $\xi < 1$.

$$\theta_2 = e^{-\xi\omega_n t}\left(A \cos \sqrt{1 - \xi^2}\,\omega_n t + B \sin \sqrt{1 - \xi^2}\,\omega_n t\right) + \theta_{2_p} \tag{32}$$

The motion resulting from this expression is shown in Figure 10 for several values of damping factor. The largest value of ξ results in the motion being damped at the least value of $\omega_n t$; the smaller the damping factor the larger the amplitude at any given time and the longer it takes the motion to damp. This trend is more easily noted by examining the time to damp to one-half amplitude.

Time to damp to one-half amplitude.- Using the exponential part of equation (32), the exponential envelope of the oscillatory motions seen in Figure 10 is obtained as

$$\theta_2 = C\, e^{-\xi\omega_n t}$$

where C is a constant. Letting θ_2 correspond to a time t_1, and θ_2' correspond to a time t_2, it is desirable to determine the time necessary to damp to a condition where

$$\theta_2' = \frac{\theta_2}{2} .$$

Thus,

$$\frac{\theta_2'}{\theta_2} = \frac{1}{2} = \frac{e^{-\xi\omega_n t_2}}{e^{-\xi\omega_n t_1}} = e^{-\xi\omega_n\left(t_2 - t_1\right)}$$

Define $\Delta t = t_2 - t_1$ as the time to damp from an amplitude of θ_2 to an amplitude of θ_2'.

$$\ln \frac{1}{2} = -\xi \omega_n \Delta t$$

and

$$\Delta t = \frac{\ln 1/2}{-\xi\omega_n} = \frac{-\ln 2}{-\xi\omega_n} = \frac{\ln 2}{\xi\omega_n} \tag{33}$$

Recalling that

$$\xi\omega_n = \frac{c}{2m} = \frac{\frac{a_2^2}{V_\infty}\frac{\partial L}{\partial \alpha} - \frac{a_2}{V_\infty}\frac{\partial M}{\partial \alpha} - \frac{\partial M}{\partial q}}{2\left(m_2 a_2^2 + J_2\right)}$$

the time to damp to one-half amplitude then becomes

$$\Delta t = \frac{2\left(m_2 a_2^2 + J_2\right)\ln 2}{\frac{a_2^2}{V_\infty}\frac{\partial L}{\partial \alpha} - \frac{a_2}{V_\infty}\frac{\partial M}{\partial \alpha} - \frac{\partial M}{\partial q}} \tag{34}$$

Spring constant.- It has been shown that a criterion for stability is that the spring constant be greater than zero. From the governing equation of motion for the decelerator rotating about its nose, equation (24), the spring constant is seen to be

$$k \equiv a_2\left(\frac{\partial L}{\partial \alpha} + D\right) - \frac{\partial M}{\partial \alpha}$$

This expression can be rewritten as

$$k = q_\infty S \bar{c}\left[\frac{a_2}{\bar{c}}\left(C_{L_\alpha} + C_D\right) - C_{m_\alpha}\right] \tag{35}$$

This can be simplified by considering the lift force in terms of normal and axial forces.

$$L = N \cos \alpha - A \sin \alpha$$

$$\frac{\partial L}{\partial \alpha} = \frac{\partial N}{\partial \alpha} \cos \alpha - N \sin \alpha - \frac{\partial A}{\partial \alpha} \sin \alpha - A \cos \alpha$$

Recalling that drag was assumed to be constant with angle of attack ($D \sim \alpha^2$), and for small angles drag force is equivalent to axial force, then $\frac{\partial A}{\partial \alpha} = 0$. The above expression is evaluated at $\alpha = 0^\circ$ to get

$$\frac{\partial L}{\partial \alpha} = \frac{\partial N}{\partial \alpha} - A$$

or

$$\frac{\partial C_L}{\partial \alpha} = \frac{\partial C_N}{\partial \alpha} - C_A$$

where C_A is equivalent to C_D at $\alpha = 0^\circ$. Substituting this into equation (35), the spring constant is found to be

$$k = q_\infty S \bar{c} \left[\frac{a_2}{\bar{c}} C_{N_\alpha} - C_{m_\alpha} \right] \tag{36}$$

To obtain some feel for the effects of the geometric and aerodynamic parameters on the spring constant, equation (36) will be examined considering a conical shaped decelerator. It is desirable to determine the difference in the spring constant for two different sizes of cone, the cone semiapex angle being a constant. It is noted that, since the semiapex angle is the same for the two cones, then

the aerodynamic characteristics, C_{N_α} and C_{m_α}, are the same. Also, the value of $a_2/\bar{c}$ would be the same.

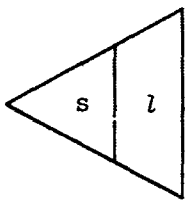

s ≡ small

l ≡ large

Writing the spring constant for both sizes of cone,

$$k_s = q_s S_s \bar{c}_s \left(\frac{a_2}{\bar{c}} C_{N_\alpha} - C_{m_\alpha} \right)$$

and

$$k_l = q_l S_l \bar{c}_l \left(\frac{a_2}{\bar{c}} C_{N_\alpha} - C_{m_\alpha} \right)$$

Thus,

$$\frac{k_s}{q_s S_s \bar{c}_s} = \frac{k_l}{q_l S_l \bar{c}_l}$$

or

$$k_l = \frac{q_l S_l \bar{c}_l}{q_s S_s \bar{c}_s} k_s \tag{37}$$

Therefore, knowing the aerodynamic spring constant of a cone having a given size and semiapex angle, the spring constant for a cone of corresponding semiapex angle but different diameter and/or dynamic pressure can be determined. For example, consider the larger cone with a diameter twice that of the small cone (i.e. $\bar{c}_l = 2\,\bar{c}_s$). Assuming the same dynamic pressure ($q_l = q_s$), it is seen that

$$k_l = \frac{S_l \bar{c}_l}{S_s \bar{c}_s} k_s$$

where

$$S_s = \frac{\pi \bar{c}_s^2}{4}$$

and

$$S_l = \frac{\pi \bar{c}_l^2}{4} = \pi \bar{c}_s^2$$

Therefore,

$$k_l = 8 k_s$$

Thus, doubling the cone diameter for a constant dynamic pressure increases the aerodynamic spring constant by a factor of eight (8). If a particular size cone were considered in equation (37), it is seen that doubling the dynamic pressure doubles the aerodynamic spring constant. This is important since the wake has a lower dynamic pressure than the freestream. If the cone aerodynamics are assumed unchanged from freestream to wake, then equation (37) predicts a lower spring constant in the wake than in freestream. Another factor to be considered concerning the spring constant is that it will remain the same magnitude regardless of center of gravity location. This can be seen from equation (36), where C_{m_α} is the aerodynamic pitching moment referenced to the decelerator center of gravity. To transfer this pitching moment to the nose of the decelerator (pin B) it is seen that

$$\left(\frac{C_{m_\alpha}}{C_{N_\alpha}}\right)_B = \left(\frac{C_{m_\alpha}}{C_{N_\alpha}}\right)_{CG} + \frac{x}{\bar{c}}$$

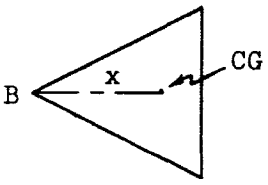

where x is the transfer distance. In the nomenclature of the present investigation this is equivalent to a_2. Thus,

$$\left(\frac{C_{m_\alpha}}{C_{N_\alpha}}\right)_B = \left(\frac{C_{m_\alpha}}{C_{N_\alpha}}\right)_{CG} - \frac{a_2}{\bar{c}}$$

or

$$C_{m_{\alpha,B}} = C_{m_{\alpha,CG}} - \frac{a_2}{\bar{c}} C_{N_\alpha}$$

From equation (36) the spring constant is therefore

$$k = - q_\infty S \bar{c} C_{m_{\alpha,B}} \tag{38}$$

It is obvious from this expression that for any body of revolution, $C_{m_{\alpha,B}}$ will be negative valued so that the spring constant will always have a positive value.

Natural angular frequency.- From equation (26) the natural angular frequency is expressed as

$$\omega_n = \sqrt{\frac{a_2\left(\frac{\partial L}{\partial \alpha} + D\right) - \frac{\partial M}{\partial \alpha}}{m_2 a_2^2 + J_2}} = \sqrt{\frac{q_\infty S \bar{c}\left(\frac{a_2}{\bar{c}} C_{N_\alpha} - C_{m_\alpha}\right)}{m_2 a_2^2 + J_2}}$$

Assuming the decelerator to be a homogeneous solid cone, the terms $m_2 a_2^2 + J_2$ can be shown to be

$$m_2 a_2^2 + J_2 = m_2 r^2 \left(\frac{16}{15} \frac{a_2^2}{r^2} + \frac{3}{20} \right) \tag{39}$$

(see reference 9)

Rewriting the expression for the natural angular frequency,

$$\omega_n = \sqrt{\frac{q_\infty S \bar{c} \left(\frac{a_2}{\bar{c}} C_{N_\alpha} - C_{m_\alpha} \right)}{m_2 r^2 \left(\frac{16}{15} \frac{a_2^2}{r^2} + \frac{3}{20} \right)}} \tag{40}$$

It can be seen from this expression that increasing the distance from the center of gravity to the apex of the cone (i.e. increasing a_2) results in corresponding decreases in the natural angular frequency. Since a homogeneous distribution of mass for the cone has been assumed, a center of gravity shift would necessitate adding mass to the system. Equation (40) shows that increasing the mass twofold would cause a decrease in ω_n by a factor of $\frac{1}{2}\sqrt{2}$.

It has been shown that if the diameter of the cone is doubled, the aerodynamic spring constant increased by a factor of 8. The effect of changing the cone diameter on the natural angular frequency will now be investigated.

Let

$$\omega_{n_s} = \sqrt{\frac{k_s}{I_s}} \quad \text{and} \quad \omega_{n_l} = \sqrt{\frac{k_l}{I_l}}$$

where

$s \equiv$ small cone

$l \equiv$ large cone

Noting that a_2/r will be the same for any diameter of a cone having the same semiapex angle, the inertia terms can be written as

$$I_s = m_s r_s^2 \left(\frac{16}{15} \frac{a_2^2}{r^2} + \frac{3}{20} \right)$$

$$I_l = m_l r_l^2 \left(\frac{16}{15} \frac{a_2^2}{r^2} + \frac{3}{20} \right)$$

Assume the cone diameter to be doubled so that $r_l = 2\, r_s$; also assume $m_l = 2\, m_s$. Thus,

$$I_l = 2\, m_s \left(4 r_s^2\right) \left(\frac{16}{15} \frac{a_2^2}{r^2} + \frac{3}{20} \right) = 8\, I_s$$

Therefore,

$$\omega_{n_l} = \sqrt{\frac{8\, k_s}{8\, I_s}} = \omega_{n_s}$$

It is seen that, if the mass of the cone is assumed to double along with the diameter of the cone, then there is no change in the natural angular frequency. On the other hand, if the mass did not double but was assumed to remain constant, then

$$\omega_{n_l} = \sqrt{2}\, \omega_{n_s}$$

Another cone property, which might be considered along with the mass, is volume. Increasing cone diameter necessarily increases cone volume, so that it might be useful to consider two cones having the same density (ρ).

Density is expressed as

$$\rho = \frac{m_s}{V_s} = \frac{m_l}{V_l}$$

where cone volume, V, is given by $\frac{1}{3} \pi r^2 h$. Writing

$$V_l = \frac{1}{3} \pi r_l^2 h_l$$

and considering the diameter and height of the cone to be doubled, it is seen that

$$r_l = 2 r_s \quad \text{and} \quad h_l = 2 h_s .$$

Thus,

$$V_l = \frac{8}{3} \pi r_s^2 h_s = 8 V_s .$$

Because of the condition of constant density, the mass of the larger cone is seen to be

$$m_l = 8 m_s .$$

This leads to $I_l = 32 I_s$, so that the natural angular frequency of the larger cone is

$$\omega_{n_l} = \sqrt{\frac{k_l}{I_l}} = \sqrt{\frac{8 k_s}{32 I_s}} = \frac{1}{2} \omega_{n_s}$$

Stability boundary.- A final comment to be made about the motion of the decelerator about its nose concerns the stability. It has been stated that a criterion for stability is that the damping be

positive values. From the governing equation of motion, equation (24), it is seen that to insure stability it is necessary that

$$\frac{a_2^2}{V_\infty}\frac{\partial L}{\partial \alpha} - \frac{a_2}{V_\infty}\frac{\partial M}{\partial \alpha} - \frac{\partial M}{\partial q} > 0$$

As mentioned previously for conical decelerator shapes, lift-curve slope is the aerodynamic parameter effected most by changing cone semiapex angle (see Figure 7) so that the boundary between stability and instability is given by

$$\frac{\partial L}{\partial \alpha} = \frac{1}{a_2}\frac{\partial M}{\partial \alpha} + \frac{V_\infty}{a_2^2}\frac{\partial M}{\partial q} \qquad (41)$$

Motion of Rod and Decelerator About Pivot Point -

Special Case No. 2

For this particular case the motion of the rod and decelerator about the pivot point (pin A) is considered,

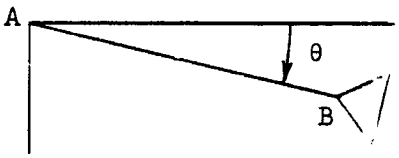

the rod and decelerator being rigidly attached at B. To obtain the equation of motion of θ it is beneficial to refer back to the coordinate system shown in Figure 3 and to set up a free-body diagram as follows:

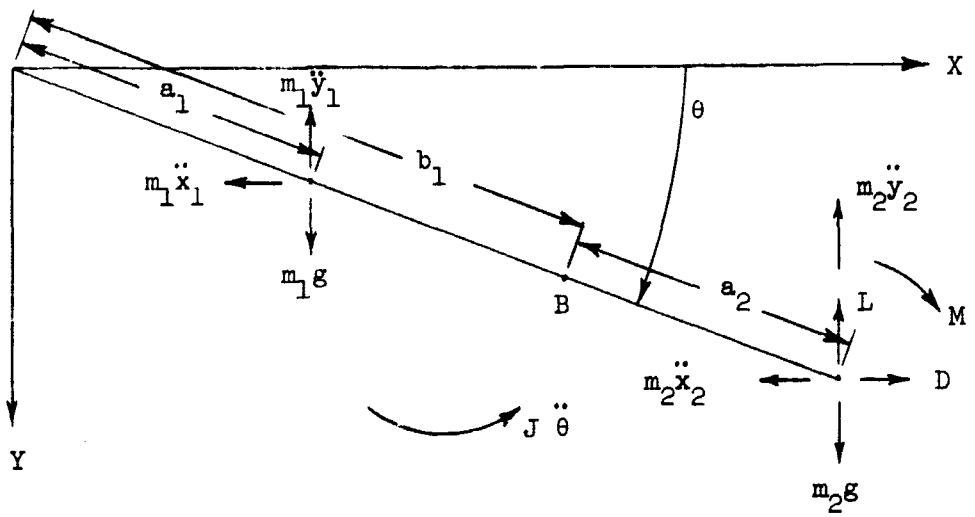

Figure 11.- Free body diagram of rod and decelerator.

The symbol J represents the sum of the mass moments of inertia of the rod and decelerator about their respective centers of gravity. In summing the moments about A, the same procedure used in section 2, page 13, is utilized here. That is, the moments are taken, the cartesian coordinates are changed to generalized coordinates, and the resulting equation is linearized. This process yields the second-order differential equation,

$$\left[m_1 a_1^2 + m_2\left(b_1 + a_2\right)^2 + J\right]\ddot{\theta} + D\left(b_1 + a_2\right)\theta + L\left(b_1 + a_2\right) - M = m_1 g a_1 + m_2 g\left(b_1 + a_2\right) \tag{42}$$

The angle of attack of the decelerator center of gravity is defined as

$$\alpha = \theta + \theta_i$$

where the induced angle, θ_i, can be shown to be

$$\theta_i = \frac{\left(b_1 + a_2\right)}{V_\infty} \dot{\theta}$$

Thus,

$$\alpha = \theta + \frac{\left(b_1 + a_2\right)}{V_\infty} \dot{\theta} \tag{43}$$

Substituting α and $\dot{\alpha}$ into the expressions for the aerodynamic lift and pitching moment yields results similar to equations (9) and (10).

$$L = \frac{\partial L}{\partial \alpha} \theta + \frac{\partial L}{\partial \alpha} \frac{\left(b_1 + a_2\right)}{V_\infty} \dot{\theta} + \frac{\partial L}{\partial \dot{\alpha}} \dot{\theta} + \frac{\partial L}{\partial \dot{\alpha}} \frac{\left(b_1 + a_2\right)}{V_\infty} \ddot{\theta} \tag{44}$$

$$M = \frac{\partial M}{\partial \alpha} \theta + \frac{\left(b_1 + a_2\right)}{V_\infty} \frac{\partial M}{\partial \alpha} \dot{\theta} + \frac{\partial M}{\partial \dot{\alpha}} \dot{\theta} + \frac{\left(b_1 + a_2\right)}{V_\infty} \frac{\partial M}{\partial \dot{\alpha}} \ddot{\theta} + \frac{\partial M}{\partial \dot{\theta}} \ddot{\theta} \tag{45}$$

where

$$\frac{\partial M}{\partial \dot{\theta}} = \frac{\partial M}{\partial q}$$

Substituting these expressions into equation (42) and collecting terms yields the following equation of motion for the one degree of freedom system:

$$\left[m_1 a_1^2 + m_2 \left(b_1 + a_2\right)^2 + J + \frac{\left(b_1 + a_2\right)^2}{V_\infty} \frac{\partial L}{\partial \dot{\alpha}} - \frac{\left(b_1 + a_2\right)}{V_\infty} \frac{\partial M}{\partial \dot{\alpha}} \right] \ddot{\theta}$$

$$+ \left[\frac{\left(b_1 + a_2\right)^2}{V_\infty} \frac{\partial L}{\partial \alpha} + \left(b_1 + a_2\right) \frac{\partial L}{\partial \dot{\alpha}} - \frac{\left(b_1 + a_2\right)}{V_\infty} \frac{\partial M}{\partial \alpha} - \frac{\partial M}{\partial \dot{\alpha}} - \frac{\partial M}{\partial q} \right] \dot{\theta}$$

$$+ \left[\left(b_1 + a_2\right) \left(D + \frac{\partial L}{\partial \alpha}\right) - \frac{\partial M}{\partial \alpha} \right] \theta = m_1 g a_1 + m_2 g \left(b_1 + a_2\right) \tag{46}$$

As previously, terms involving $\frac{\partial L}{\partial \dot{\alpha}}$ and $\frac{\partial M}{\partial \dot{\alpha}}$ are neglected and this equation reduces to

$$\left[m_1 a_1^2 + m_2\left(b_1 + a_2\right)^2 + J\right] \ddot{\theta} + \left[\frac{\left(b_1 + a_2\right)^2}{V_\infty} \frac{\partial L}{\partial \alpha} - \frac{\left(b_1 + a_2\right)}{V_\infty} \frac{\partial M}{\partial \alpha} - \frac{\partial M}{\partial q}\right] \dot{\theta}$$

$$+ \left[\left(b_1 + a_2\right)\left(D + \frac{\partial L}{\partial \alpha}\right) - \frac{\partial M}{\partial \alpha}\right] \theta = m_1 g a_1 + m_2 g \left(b_1 + a_2\right) \qquad (47)$$

The particular solution is found from this equation to be

$$\theta_p = \frac{m_1 g a_1 + m_2 g \left(b_1 + a_2\right)}{\left[\left(b_1 + a_2\right)\left(D + \frac{\partial L}{\partial \alpha}\right) - \frac{\partial M}{\partial \alpha}\right]} \qquad (48)$$

This can be simplified somewhat by recalling that

$$\frac{\partial L}{\partial \alpha} = \frac{\partial N}{\partial \alpha} - A \quad \text{at} \quad \alpha = 0^\circ$$

Thus,

$$\theta_p = \frac{m_1 g a_1 + m_2 g\left(b_1 + a_2\right)}{\left[\left(b_1 + a_2\right)\frac{\partial N}{\partial \alpha} - \frac{\partial M}{\partial \alpha}\right]} \qquad (49)$$

The homogeneous equation is given by

$$\left[m_1 a_1^2 + m_2 \left(b_1 + a_2\right)^2 + J\right] \ddot{\theta} + \left[\frac{\left(b_1 + a_2\right)^2}{V_\infty} \frac{\partial L}{\partial \alpha} - \frac{\left(b_1 + a_2\right)}{V_\infty} \frac{\partial M}{\partial \alpha} - \frac{\partial M}{\partial q}\right] \dot{\theta}$$

$$+ \left[\left(b_1 + a_2\right)\left(D + \frac{\partial L}{\partial \alpha}\right) - \frac{\partial M}{\partial \alpha}\right] \theta = 0 \qquad (50)$$

which has the same form as equations (22) and (23), where

$$\Delta t = \frac{2\left[m_1 a_1^{\,2} + m_2\left(b_1 + a_2\right)^2 + J\right] \ln 2}{\left[\frac{\left(b_1 + a_2\right)^2}{V_\infty}\frac{\partial L}{\partial \alpha} - \frac{\left(b_1 + a_2\right)}{V_\infty}\frac{\partial M}{\partial \alpha} - \frac{\partial M}{\partial q}\right]} \tag{51}$$

Spring constant.- From equation (50) the spring constant can be written as

$$k = \left(b_1 + a_2\right)\left(D + \frac{\partial L}{\partial \alpha}\right) - \frac{\partial M}{\partial \alpha}$$

Nondimensionalizing this expression,

$$k = q_\infty S\,\bar{c}\left[\frac{\left(b_1 + a_2\right)}{\bar{c}}\left(C_D + C_{L_\alpha}\right) - C_{m_\alpha}\right]$$

where $C_{L_\alpha} = \frac{\partial C_L}{\partial \alpha}$ and $C_{m_\alpha} = \frac{\partial C_m}{\partial \alpha}$. This can be written as

$$k = q_\infty S\,\bar{c}\left[\frac{\left(b_1 + a_2\right)}{\bar{c}}\,C_{N_\alpha} - C_{m_\alpha}\right] \tag{52}$$

The spring constant is seen to be positive valued at all times, the magnitude of which remains invariant with center of gravity location. Similar to the argument presented in describing the motion of the decelerator about its nose, equation (38), the spring constant in the above expression can be written as

$$k = -\,q_\infty S\,\bar{c}\,C_{m_{\alpha,A}} \tag{53}$$

where $C_{m_{\alpha,A}}$ is the aerodynamic pitching moment referenced to the point of rotation, pin A. The magnitude of $C_{m_{\alpha,A}}$ (and thus the

spring constant) in this expression is larger than $C_{m_{\alpha,B}}$ in equation (38) by the amount $-\frac{b_1}{\bar{c}} C_{N_\alpha}$.

To evaluate the spring constant for two conical shaped decelerators having the same semiapex angle, the spring constant is written as follows:

$$k_s = q_s S_s \bar{c}_s \left[\frac{\left(b_{1_s} + a_{2_s}\right)}{\bar{c}_s} C_{N_\alpha} - C_{m_\alpha} \right]$$

$$k_l = q_l S_l \bar{c}_l \left[\frac{\left(b_{1_l} + a_{2_l}\right)}{\bar{c}_l} C_{N_\alpha} - C_{m_\alpha} \right]$$

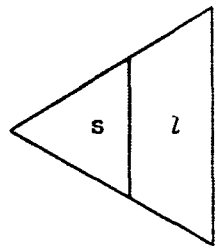

where C_{N_α} and C_{m_α} are the same for the two cones. Assume

$$\frac{b_{1_s} + a_{2_s}}{\bar{c}_s}$$

is equivalent to

$$\frac{b_{1_l} + a_{2_l}}{\bar{c}_l}$$

so that

$$k_l = \frac{q_l S_l \bar{c}_l}{q_s S_s \bar{c}_s} \tag{54}$$

which is the same expression obtained in equation (37). Considering the larger cone to have twice the diameter of the small cone, the comments made concerning equation (37) are appropriate here. However, there is a condition placed on the length of the rod by the expression

$$\frac{b_{1_s} + a_{2_s}}{\bar{c}_s} = \frac{b_{1_l} + a_{2_l}}{\bar{c}_l} \quad .$$

Since

$$\frac{a_{2_s}}{\bar{c}_s} = \frac{a_{2_l}}{\bar{c}_l} \quad ,$$

then

$$\frac{b_{1_s}}{\bar{c}_s} = \frac{b_{1_l}}{\bar{c}_l} \quad .$$

Therefore, when the diameter of the cone is doubled $\left(\bar{c}_l = 2\ \bar{c}_s\right)$, the length of the rod for the larger cone must be twice that for the smaller cone $\left(b_{1_l} = 2\ b_{1_s}\right)$ in order that equation (54) be valid.

Natural angular frequency.- From equation (50) the natural angular frequency is expressed as

$$\omega_n = \sqrt{\frac{q_\infty S\ \bar{c}\left[\frac{\left(b_1 + a_2\right)}{\bar{c}} C_{N_\alpha} - C_{m_\alpha}\right]}{m_1 a_1^2 + m_2\left(b_1 + a_2\right)^2 + J}} \tag{55}$$

Assuming the rod and cone to be homogeneous solids, the mass moment of inertia (J) about their centers of gravity can be written as

$$J = J_1 + J_2$$

where

$$J_1 = \frac{1}{12} m_1 b_1^2$$

and

$$J_2 = \frac{3}{20} m_2 \left(r^2 + \frac{h^2}{4}\right)$$

Letting $m_1 = m_2$, which isn't unrealistic for a decelerator system, $h = \frac{4}{3} a_2$, and $a_1 = \frac{b_1}{2}$, the natural angular frequency can be expressed as

$$\omega_n = \sqrt{\frac{q_\infty S \bar{c}\left[\frac{(b_1 + a_2)}{\bar{c}} C_{N_\alpha} - C_{m_\alpha}\right]}{\frac{1}{4} m_2 b_1^2 + m_2 (b_1 + a_2)^2 + \frac{1}{12} m_2 b_1^2 + \frac{3}{20} m_2 \left(r^2 + \frac{4}{9} a_2^2\right)}} \qquad (56)$$

From this it is seen that increasing dynamic pressure causes an increase in ω_n, while increasing mass and/or the distance of mass from the rotation point (pin A) causes corresponding decreases in ω_n. Assuming the length of the rod to be much greater than the distance from the cone CG to the nose of the cone $(b_1 >> a_2)$ will not seriously alter these trends so that equation (56) may be reduced to

$$\omega_n = \sqrt{\frac{q_\infty S \bar{c}\left[\frac{b_1}{\bar{c}} C_{N_\alpha} - C_{m_\alpha}\right]}{m_2 r^2 \left(\frac{4}{3} \frac{b_1^2}{r^2} + \frac{3}{20}\right)}} \qquad (57)$$

The effect of doubling the cone diameter can be seen by letting

$$\omega_{n_s} = \sqrt{\frac{k_s}{I_s}} \quad \text{and} \quad \omega_{n_l} = \sqrt{\frac{k_l}{I_l}}$$

where

$$I_s = m_s r_s^2 \left(\frac{4}{3} \frac{b_{l_s}^2}{r_s^2} + \frac{3}{20} \right)$$

$$I_l = m_l r_l^2 \left(\frac{4}{3} \frac{b_{l_l}^2}{r_l^2} + \frac{3}{20} \right)$$

It is noted that letting $\frac{b_l}{r}$ be the same for the two cones leads to the same remarks made in the previous section (see page 47) concerning the effects of doubling the cone diameter on the natural angular frequency. With $r_l = 2\, r_s$, it is seen that

$$\frac{b_{l_l}}{r_l} = \frac{b_{l_s}}{r_s} \quad \text{or} \quad b_{l_l} = 2\, b_{l_s} \; .$$

The reader will note that this is the same condition concerning the length of the rod which resulted during the previous discussion of the effects of doubling cone diameter on the spring constant.

Stability boundary.- Since the spring constant is always positive, it is only necessary for the damping to be positive to insure stability for the dynamic system described by equation (47). Thus, the boundary between stability and instability is represented by

$$\frac{\left(b_1 + a_2\right)^2}{V_\infty} \frac{\partial L}{\partial \alpha} - \frac{\left(b_1 + a_2\right)}{V_\infty} \frac{\partial M}{\partial \alpha} - \frac{\partial M}{\partial q} = 0 \qquad (58)$$

In terms of lift-curve slope this becomes,

$$\frac{\partial L}{\partial \alpha} = \frac{1}{\left(b_1 + a_2\right)} \frac{\partial M}{\partial \alpha} + \frac{V_\infty}{\left(b_1 + a_2\right)^2} \frac{\partial M}{\partial q} \tag{59}$$

The similarity between this stability boundary and that obtained for the cone rotating about its nose, equation (41), should be noted.

VII. CONCLUDING REMARKS

A preliminary investigation has been undertaken to theoretically determine the geometric and aerodynamic parameters which have the greatest influence on the stability and performance of the nonporous towed decelerator. To aid in this endeavor a mathematical model was generated to describe the flexible tow line - decelerator dynamical system as a rigid two-body problem. The resulting second-order governing differential equations of motion were used to obtain the characteristic equation (quartic) describing the coupled motions of the two bodies. Evaluation of the coefficients of the quartic yielded expressions which illustrate when the dynamical system is unquestionably unstable.

The two single-degree of freedom cases investigated were the motion of the decelerator about its nose and the motion of the rod and decelerator about the pivot point. For both of these cases expressions were derived for the natural angular frequency, damping factor, steady-state solution, and time to damp to one-half amplitude. Specific comments were made concerning a conical shaped decelerator to illustrate some of the geometric and aerodynamic parameters affecting the spring constant and the natural angular frequency. The boundary between stability and instability was obtained for these two single-degree of freedom cases.

VIII. REFERENCES

1. Charczenko, Nickolai, and McShera, John T.: Aerodynamic Characteristics of Towed Cones Used as Decelerators at Mach Numbers From 1.57 to 4.65. NASA TN D-994, December 1961.

2. Charczenko, Nickolai: Aerodynamic Characteristics of Towed Spheres, Conical Rings, and Cones Used as Decelerators at Mach Numbers From 1.57 to 4.65. NASA TN D-1789, April 1963.

3. MacNeal, Richard H.: The Flutter of Towed Rigid Decelerators. NASA CR-766, May 1967.

4. Reding, J. Peter and Ericsson, Lars E.: Loads on Bodies in Wakes. AIAA Aerodynamic Deceleration Systems Conference, September 1966.

5. Myklestad, N. O.: Fundamentals of Vibration Analysis. McGraw-Hill Book Company, Inc., New York, 1956.

6. Campbell, James F.: Supersonic Aerodynamics of Large-Angle Cones. Prospective NASA TN.

7. Allen, H. Julian: Motion of a Ballistic Missle Angularly Misaligned With the Flight Path Upon Entering the Atmosphere and its Effect Upon Aerodynamic Heating, Aerodynamic Loads, and Miss Distance. NACA TN -4048, October 1957.

8. Wylie, C. R., Jr.: Advanced Engineering Mathematics. McGraw-Hill Book Company, Inc., New York, 1951, page 625.

9. Hudson, Ralph G.: The Engineers' Manual. Second Edition, John Wiley and Sons, Inc., London, 1957, page 93.

IX. VITA

The author was born [redacted] in [redacted]. He was graduated from Lewisburg Joint High School, Lewisburg, Pennsylvania in 1959 and received a Bachelor of Science Degree in Aerospace Engineering from Mississippi State University in 1963. Since graduation from college, he has been employed as an Aerospace Technologist by the National Aeronautics and Space Administration at Langley Research Center, Virginia.